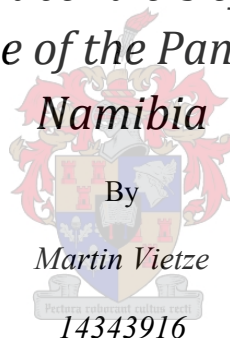




UNIVERSITEIT  
STELLENBOSCH  
UNIVERSITY

*Geology and emplacement controls of the Stinkbank granite in  
the south Central Zone of the Pan-African Damara Belt,  
Namibia*



By

*Martin Vietze*

14343916

*Thesis presented in partial fulfillment of the requirements for the degree of*

**Master of Science**

At the University of Stellenbosch

2009

Supervised by Prof. Alex Kisters and Prof. Gary Stevens

## **DECLARATION**

I, the undersigned, hereby declare that the work presented in this thesis is my own original work and that I have not previously in its entirety or in part submitted it at any other university for a degree.

Signature:.....

Date: 1 December 2009

## **ABSTRACT**

Regional mapping of the Stinkbank granite in the south Central Zone of the Damara Belt, focused on an area of ca. 150 km<sup>2</sup> in the SW parts of the granite along well exposed sections of the Khan River to the SW of the town of Usakos. The granite forms part of the regionally widespread granite suite of Salem-type granites that intruded at ca. 550-540 Ma into amphibolite-facies rocks of the Damara Supergroup. The Stinkbank granite is intrusive into the regional-scale, NE-trending D<sub>2</sub> Kransberg syncline, cored by schists of the Kuiseb Formation and surrounded by marble units of the Karibib Formation.

The granite comprises three major lithotypes that have intruded in sequence. The earliest granites are represented by biotite-rich megacrystic granites, followed by leucocratic megacrystic granites and a final stage of voluminous, garnetiferous and tourmaline-bearing, medium-grained leucogranites. Contact relationships with the wall rocks are, for the most part, concordant, documenting the largely sheet-like geometry of the granites. Internal contacts between different granite phases are well preserved and indicate that the granites have intruded as shallowly-dipping, largely concordant sheets. Intrusive contact relationships and petrographic and geochemical characteristics indicate that each of the three major granite phases represented a distinct emplacement pulse. Successive emplacement of the granite sheets point to the assembly of the Stinkbank granite from the top down, with younger sheets intruding structurally below earlier emplaced granite sheets. This has created a pseudostratigraphy within the Stinkbank granite. The mapping of the internal contacts shows that the granite sheets were progressively folded into NE-trending, upright folds, parallel to D<sub>2</sub> folds in the surrounding wall rocks. NE-trending magmatic and solid-state foliations in all granite phases are axial planar to the folds and underline the syntectonic emplacement of the Stinkbank granite during the D<sub>2</sub> NW-SE subhorizontal shortening.

Based on the intrusive relationships and the progressive deformation of granite phases, an intrusive sequence can be developed for the Stinkbank granite. The earliest granite phases were emplaced during the onset of the regional D<sub>2</sub> deformation, parallel to the subhorizontal bedding. Continued granite sheeting led to the vertical growth of the sheet-like granite and bending of the wall rocks above the inflating granite sheets, leading to the laccolithic geometry of the SW parts

of the Stinkbank granite. Progressive deformation, folding of the granite sheets and fold amplification resulted in fold interference patterns in the SW parts of the Stinkbank granite.

The Stinkbank granite represents a mid-crustal granite with well-preserved granite sheeting that was assembled during regional deformation. Granite sheeting and progressive deformation illustrate the interplay between (1) regional strains, and (2) the orientation and presence of pre-existing wall-rock anisotropies (bedding) and their significance for the magmatic assembly and progressive deformation of the granite.

## UITTREKSEL

*Regionale kartering van die Stinkbank graniet in die suidelike Sentrale Sone (sSS) van die Damara Gordel. Die studie fokus op die area van ongeveer 150 km<sup>2</sup> in die SW dele van die graniet, langs n goed blootgestelde seksie van die Khan Rivier, SW van Usakos. Die graniet vorm deel van n wydverspreide suite van Salem- tipe graniete wat tussen 550-540 Ma in die amfiboliet fasies gesteentes van die Damara Supregroep ingedring het. Die Stinkbank graniet kom voor in regionale –skaal , NE – neigende D<sub>2</sub> Kransberg Sinklinorium, wat bestaan uit skis van die Kuiseb Formasie en marmer van die Karibib Formasie.*

*Die graniet bestaan uit drie hoof fases wat in volgorde ingedring het. Die oudste graniet is die biotiet-ryke megakristiese graniet, gevolg deur die leukokratiese megakristiese graniet en laastens die leukograniet. Kontak verhoudings met die wandgesteentes is grootendeels konkordant en dit dui op die feit dat die graniet uit lae bestaan. Die interne kontakte tussen die verskillende graniete is goed preserveer en dui aan dat die graniete voorkom as vlak lêende lae. Kontakverhoudings, petrografie en geochemiese karakteristieke dui aan dat elk van die drie tipes graniet uniek is. Die volgorde van intrusie van die Stinkbank graniet het voorgekom van bo na onder. Dit het n “skyn-stratigrafie” tot gevolg gehad. Kartering van die interne kontakte tussen die graniete het getoon dat die graniet lae is deurentyd gevou na NE- neigende, regop voue, parallel aan die D<sub>2</sub> voue in die omringende wandgesteentes. NE- neigende magmatiese en soliede stadium foliasies in al die graniete is asvlak planêr aan die voue en dui ook op die syn-tektoniese intrusie van die Stinkbank graniet gedurende die D<sub>2</sub> , NW-SE subhorisontale verkorting.*

*Intrusiewe verhoudings en die progressiewe deformatsie van die graniet, dui dat n volgorde verkry kan word vir die Stinkbank graniet. Die oudste graniet fase het ingedring gedurende die begin van die streekse D<sub>2</sub> deformatsie, parallel aan die subhorisontale gelaagdheid. Aanhoudende graniet-lae intrusies het gely tot die groei van n laag-ryke graniet en die buiging van die omliggende wangesteentes om dit n lakoliet vorm te gee in die SW dele van die Stinkbank graniet. Progressiewe deformatsie, vouing van graniet lae en vergroting van voue het tot vou-interferensie patrone in die SW dele van die Stinkbank graniet tot gevolg gehad.*

*Die Stinkbank graniet stel n middel- kors graniet met goed gepreserveerde gelaagdheid, wat gedurende regional deformatsie ingedring het, voor. Graniet lae en progressiewe deformatsie illustreer die verhouding tussen (1) regionale spanning en (2) die orientasie en teenwoordigheid van voorafbestaande wandgesteente anisotropie (gelaagdheid) en hulle belangrikheid vir die opbou en deformatsie van die graniet.*

## ACKNOWLEDGEMENTS

- Professor Alex Kisters, for TIME, effort, energy, enthusiasm, inspiration and even more time. It has been an honour to work with this brilliant geologist and teacher. Thanks for absolutely everything, I owe you more than a case of good whiskey.
- Navachab gold mine, Frik Badenhorst, for generously funding the project and supplying the necessary 4X4 vehicles and logistic support.
- To my parents, thank you for giving me the opportunity to study for six long years. I appreciate all the sacrifices you have made to get me to where I am.
- My MSc lab buddies, thanks for the hours and hours of uplifting chats, coffee breaks and brazen visits.
- Chris, for the 2 years and especially those three months in the town of Karibib. 1913 will forever live on in my mind.
- Prof. Gary Stevens for providing some extra logistical and financial support.

## **CONTENTS**

• <i>Declaration</i>	<i>i</i>
• <i>Abstract</i>	<i>ii</i>
• <i>Uittreksel</i>	<i>iv</i>
• <i>Acknowledgements</i>	<i>v</i>
• <i>Contents</i>	<i>vi</i>
• <i>Appendices</i>	<i>ix</i>
<b>1. INTRODUCTION</b>	<b>1</b>
<i>1.1 The study area</i>	<i>2</i>
<i>1.2 Aims of the study</i>	<i>4</i>
<i>1.3 Methodology</i>	<i>5</i>
<b>2. GEOLOGICAL SETTING</b>	<b>7</b>
<i>2.1 The Damara Orogen</i>	<i>7</i>
<i>2.1.1 Introduction</i>	<i>7</i>
<i>2.1.2 Tectonostratigraphic Evolution of the CZ in the Damara Belt</i>	<i>9</i>
<i>2.1.3 Granite plutonism in the CZ of the Damara belt</i>	<i>13</i>
<i>2.2 The Stinkbank granite-previous work</i>	<i>14</i>
<b>3. LITHOSTRATIGRAPHY AND FIELD RELATIONS</b>	<b>15</b>
<i>3.1 Introduction</i>	<i>15</i>
<i>3.2 Pre- Damaran Basement</i>	<i>18</i>
<i>3.3 Damara Sequence</i>	<i>18</i>
<i>3.3.1 Rocks of the Nosib Group</i>	<i>18</i>

3.3.2 <i>Swakop Group</i>	19
3.3.2.1 <i>Karibib Formation</i>	19
3.3.2.2 <i>Kuiseb Formation</i>	21
3.3.3 <i>Petrography</i>	23
3.4 <i>Intrusive Rocks</i>	24
3.4.1 <i>Granitic and pegmatitic sills and dykes intrusions</i>	24
3.4.2 <i>Dolerite dykes</i>	24
<b>4. STRUCTURAL GEOLOGY</b>	<b>25</b>
4.1 <i>Introduction</i>	25
4.2 <i>Primary Bedding (<math>S_0</math>)</i>	27
4.3 <i>Tectonic Fabrics</i>	28
4.3.1 <i>Foliation (<math>S_1</math>)</i>	28
4.3.2 <i>Foliation (<math>S_2</math>)</i>	28
4.3.3 <i>Lineations (<math>L_{2a}</math>)</i>	28
4.4 <i>Folding</i>	29
4.4.1 <i>F1 Folding</i>	29
4.4.2 <i>F2 Folding</i>	29
4.5 <i>Domain 1</i>	32
4.5.1 <i>Wall-rock Structure</i>	32
4.6 <i>Domain 2</i>	39
4.6.1 <i>Wall-rock Structure</i>	39
<b>5. THE STINKBANK GRANITE AND RELATED PHASES</b>	<b>44</b>
5.1 <i>Field appearance and distribution of granite varieties within the Stinkbank granite</i>	44

5.1.1 <i>Leucogranite</i>	44
5.1.2 <i>Leucocratic megacrystic Stinkbank granite</i>	48
5.1.3 <i>Biotite-rich, megacrystic Stinkbank granite</i>	49
5.1.4 <i>Sill- and dyke-like intrusions</i>	51
5.2 <i>Fabric development in the Stinkbank granite</i>	55
5.3 <i>Internal architecture of the Stinkbank granite</i>	60
5.3.1 <i>Intrusive and relative age relationships</i>	60
5.3.2 <i>Contact relationships and granite geometries</i>	61
5.3.3 <i>Granite Pseudostratigraphy</i>	71
5.3.4 <i>Granite- Wall rock contacts</i>	72
<b>6. GEOCHEMISTRY</b>	<b>77</b>
6.1 <i>Results</i>	79
<b>7. DISCUSSION</b>	<b>83</b>
7.1 <i>Regional strains</i>	83
7.2 <i>Intrusive sequence and sheet-like geometry of the Stinkbank granite</i>	83
7.3 <i>Synkinematic timing of granite plutonism and deformation of the Stinkbank granite</i>	86
7.4 <i>The Stinkbank granite as a laccolith</i>	87
7.5 <i>The role of granite sheeting for the assembly of the Stinkbank granite</i>	89
7.6 <i>Emplacement of the Stinkbank granite – towards an overall model</i>	94
7.7 <i>Regional controls of emplacement</i>	98

<b>8. CONCLUSIONS</b>		<b>100</b>
<b>9. REFERENCES</b>		<b>102</b>
<b>APPENDIX</b>		<b>111</b>
APPENDIX 1	<i>Geological map of the Kransberg Syncline, south Central Zone, Damara Belt, Namibia</i>	
APPENDIX 2	<i>Form line map illustrating major fold structures within the Kransberg Syncline, south Central Zone, Damara Belt, Namibia</i>	

## 1. INTRODUCTION

Granites represent the main process of crustal differentiation (*Taylor and McLennan, 1985*). Lower crustal melting at elevated temperatures yields granitic melts that ascend through the crust, concentrating otherwise incompatible elements in the melts that are then emplaced at shallower crustal levels (*Brown, 1994a, 2007*). For decades, the processes of granite formation have been the domain of mainly petrologists and geochemists. The scale of melt transfer, however, resulting in large batholithic complexes that may, in places, combine thousands of cubic kilometres of magma, raises the question as to how this melt transfer and the final emplacement is accomplished in essentially subsolidus, brittle crust. This is where, some 15 to 20 years ago, structural studies have addressed the questions of melt transfer and granite emplacement in the continental crust (*e.g. Hutton 1988; Clemens and Mawer 1992; Paterson and Fowler, 1993; Brown and Solar, 1998b; Petford et al., 2000; Vigneresse and Clemens, 2000; Glazner and Bartley, 2006*).

This study focuses mainly on the concluding part of the transport process and the final emplacement of granitic melts studying the Pan-African Stinkbank granite in the Damara Belt of central Namibia. Emplacement implies the creation of space for the intruding magma. The creation of space is commonly achieved through a combination of processes. In syntectonic granite plutons, the deforming wall rocks may provide the space, either during regional extension or, locally, in jog geometries along e.g. shear zones or in fold structures (*Vigneresse, 1995; Brown and Solar, 1998a, b; McCaffrey, 1992 Archanjo et al., 1999*). On a more local scale, space may be created by the magma itself. The internal magma pressure may push and displace the wall rocks and mechanisms such as the uplift of the roof rocks of plutons, floor depression below granites and/or the stoping of wall rocks are increasingly documented features that accommodate the intruding magma (*e.g. Cruden, 1998 ; Pitcher, 1997; McCaffrey & Petford, 1997; Clemens and Petford, 2000; Vigneresse & Clemens 2000*). Moreover, recent works have shown that granite plutons are not the steep-sided, plug-shaped bodies as which they are commonly depicted on regional sections and maps. In 3D, most granites can be shown to be rather sheet like, forming either bedding/foliation parallel sills (*e.g. Hutton, 1988*) or laccoliths or lopoliths (*Horsman et al., 2005*). In both cases, pre-existing anisotropies in the wall rocks and the regional strain/stress field exert important controls on the emplacement of the plutons

(*Paterson and Fowler, 1993; Brown and Solar, 1998a, b;*). Lastly, the paradigm of granites ascending and being emplaced as large, singular magma bodies seems no longer tenable (*e.g. Coleman et al., 2004; Glazner et al., 2004*). Instead, most granites seem to have been assembled from numerous magma batches. These individual batches may be difficult to recognize at the emplacement site, but the progressive amalgamation of melt batches to form granites is discernable particularly along granite margins (*e.g. Westraat et al., 2005*), through high-resolution geochronology (*e.g. Glazner et al., 2004*) or isotopic fingerprinting.

### ***1.1 The study area***

The Pan-African Damara Belt in central Namibia is one of the world's classic granite terrains with over 75000km<sup>2</sup> of the Central Zone of the belt underlain by granite (*Miller, 1983; 2008*). Most studies have focused on the petrogenesis of the granites, geochemical and isotope geochemical signatures, possible source rocks and the timing of plutonism with respect to the regional tectonism (*Jacob, 1974; Sawyer, 1976; Miller, 1983; Jung et al., 1998, 2001; Jung and Mezger, 2001, 2003; Jacob et al. 2000; Tack et al., 2002*) However, there are only few studies that have dealt with the actual structural controls and mechanisms of granite emplacement. Amongst these few studies, a number of different emplacement models have been suggested. Regional maps and cross-section show granite plutons mainly as steep-sided, sharply cross-cutting plugs (*Smith, 1965*). The close association of granites with regional-scale fold structures and certain stratigraphic levels has been suggested to indicate a structural control of emplacement (*Miller, 1983*), whereas concordant wall-rock granite relationships have also been invoked to point to granite diapirism and ballooning (*Kröner, 1982*). More recent studies emphasize the often sheeted internal structure and sheet-like geometry of many granites (*Ameglio et al., 2000; Johnson, 2005; Johnson et al., 2006a; Miller, 2008*).

The project focuses on the geology and emplacement controls of the Stinkbank granite. The Stinkbank granite is situated in the south Central Zone of the Pan-African Damara Belt in central Namibia, and covers an area of altogether ca. 600km<sup>2</sup>, forming part of the regionally widespread group of so-called Salem-type granites (*SACS, 1980; Marlow, 1983; Miller 1983; Jung et al., 1998; Jacob et al., 2000; Tack et al., 2002*). The term Salem-type granite describes a common association of distinct granite types in the Damara Belt. These granites form large, composite

batholithic complexes and are typically emplaced at a certain stratigraphic level within the Damara Supergroup (Jacob, 1974; Miller, 1983; Marlow, 1983).

Exposure of the Stinkbank granite is very good in the SE and S parts of the granite with, in places, near-continuous outcrops of large granite platforms and wall rocks of the Damara Supergroup. Contact relationships between the Stinkbank granite and country rocks of the Damara Supergroup range from seemingly concordant to highly discordant and also from sharp to gradual. Large, km-scale wall-rock xenoliths are clearly discernable on satellite photos in the central parts of the granite. The SW termination of the Stinkbank granite is sharp with seemingly concordant granite-wall-rock contact relationships, whereas the NW termination is gradual and somewhat indistinct, showing granite stockworks and intrusive breccias in metaturbidites of the Kuiseb Formation. For this project, the better exposed SW extent of the granite was mapped along a ca. 20 km long and 7 km wide strip, straddling the mostly dry riverbed of the Khan River. The area stretches from the SE of the town of Usakos (22° 00'S; 15° 35'E) to the farms Safier and Namibfontein (Figure 1.1).

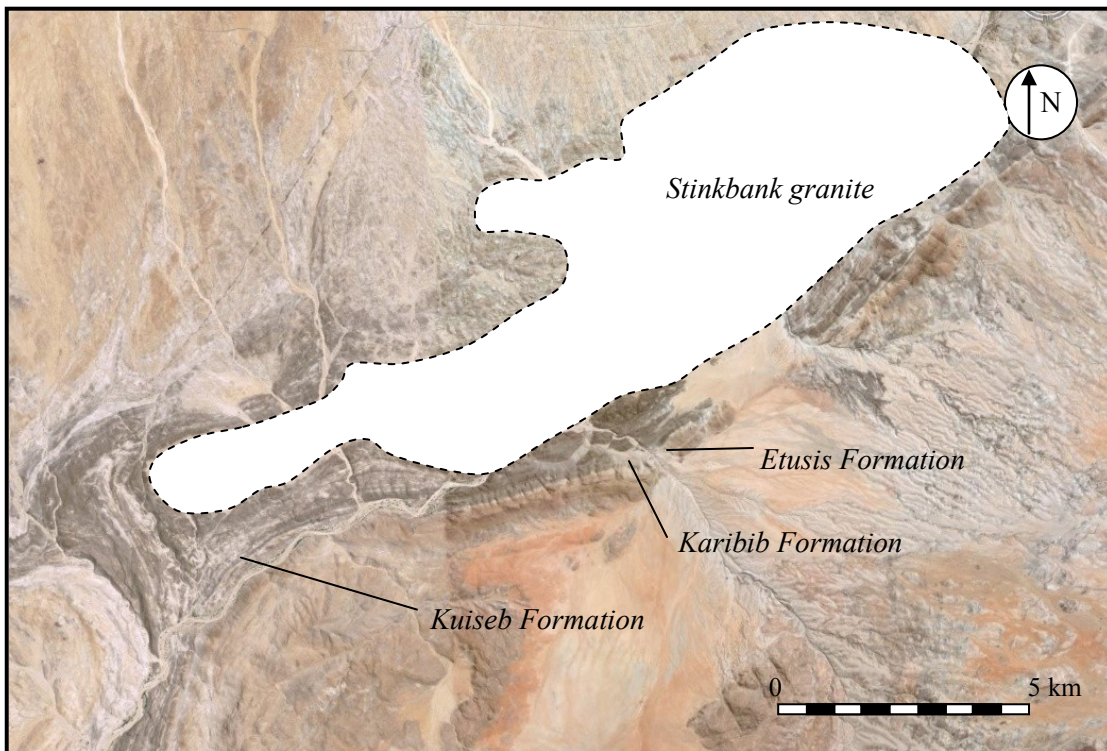


Figure 1.1, Google Earth image of the study area and surroundings. The SW parts of the Stinkbank granite studied in this project are delineated by the dashed line and shaded area. Wall rocks of the Etusis-, Karibib- and Kuiseb Formations are also indicated on the image. The area is 20 km in strikelength (NE-SW) and 7km in width.

## ***1.2 Aims of the study***

The aims of the present project are as follows:

(1) Describe the overall geometry of the Stinkbank granite as a typical Salem-type granite. Granite wall-rock contact relationships are well exposed in the SW parts of the granite and can be traced for tens of kilometres, despite the lack of prominent topography. This will be used to analyze the processes of granite emplacement and relationships to the likely 3-D geometry of the granite.

(2) Identify and describe the relationship between the internal structure of the pluton, including magmatic and/or solid-state fabrics, folding and/or boudinage of granite phases, with strains and fabrics/structures in the wall-rocks on a local scale, i.e. in the contact zones, as well as on a regional scale. In general, previous works have emphasized the syn- to post-tectonic timing of Salem-type granites (*Martin, 1965; Jacob, 1974; Miller 1978, 1983; Johnson et al., 2006a; Jung et al., 1998; Smith, 1965*). Can regional strains be identified within the pluton or, vice versa, have the granites superimposed local and emplacement-related strains onto the wall rocks? Can progressive regional deformation be traced in successively emplaced granite phases and are all granite phases syn-tectonic?

(3) Document the likely heterogeneity of the Stinkbank granite as a typical Salem-type granite. This includes the description of the main petrographic characteristics and differences, the bulk geochemistry of the granites, the geometry of intrusive phases and intrusive contacts and, as such, timing relationships between the main granite phases. The geological data is to be presented on a detailed geological map of the southern and SW portions of the Stinkbank granite.

(4) Discuss the possible controls on the regional stratigraphic and structural position of the Salem-type granites within the Damara Supergroup, i.e. the consistent, orogen-wide level of emplacement above the interface between marbles of the Karibib Formation and in regional-scale synformal structures.

### ***1.3 Methodology***

Fieldwork was carried out in three main field seasons, including an initial, three-week reconnaissance mapping in March 2008, a main three-month field season between June and October 2008, and final work over a period of two weeks in March 2009. Mapping was undertaken based on imagery obtained from Google Earth and locations were georeferenced with a handheld GPS (Garmin GPS 80). The scale of mapping is variable and depends on the complexity of features recorded in the field. Structural readings were taken with a Breithaupt structural compass. In this thesis, all planar readings are given as the dip azimuth and dip angle, whereas linear elements are given as the plunge direction and plunge.

All structural data are plotted as equal area projections and into the lower hemisphere using the programme StereoNett, devised by Johannes Duyster, Ruhr University, Bochum, Germany. Geological and structural maps were digitized using ArcGIS (9.2). Adobe Illustrator (CS2) was used for draughting the cross sections and detailed outcrop maps and line drawings.

Samples of the main lithological units were collected and processed for geochemical analyses and petrographic and microstructural studies. The geochemical analyses were done in the geochemical laboratory of the University of Hamburg and the technical specifications are given in Chapter 6.

*SW*

*NE*



*Figure 1.2*, Panorama of the field area, looking from the Etusis Formation in the SE across the Khan River valley (middleground) and the Stinkbank granite (center)

## **2. GEOLOGICAL SETTING**

### **2.1 The Damara Orogen**

#### *2.1.1 Introduction*

The Damara Orogen in southern Africa consists of the Kaoko, Damara, and Gariep Belts. It was formed as a result of the initial rifting and subsequent convergence and collision of cratonic blocks, namely the Kalahari and Congo Cratons in Africa, and Archaean to Mesoproterozoic equivalents in South America between ca. 750-500 Ma (*Miller, 1983; Stanistreet et al., 1991*). The Damara Belt forms the NE trending, so-called inland branch of the larger Damara Orogen. The Belt records a complete history from rifting and associated rift sedimentation and volcanism, via an oceanic stage and marine sedimentation through to convergence and final collision (*Miller, 1983; Porada, 1989*). It can be divided into eight main tectonostratigraphic zones (*Miller, 1983*). They are arranged parallel to the axis of orogen, including the *NP*: Northern Platform; *NZ*: Northern Zone; *NCZ*: Northern CZ; *SCZ*: Southern CZ; *OLZ*: Okahandja Lineament Zone; *SZ*: Southern Zone; *SMZ*: Southern Margin Zone; *SF*: Southern Foreland (Figure 2.1).

The NZ is N-verging fold-and-thrust belt with low metamorphic grade. The CZ is characterized by an abundance of granites and the presence of high grade metamorphic rocks. It is subdivided into a southern (south CZ, *sCZ*) and a northern part (north CZ, *nCZ*) according to the prevailing presence of the upper and lower stratigraphy of the Damara Supergroup, respectively. The *SZ* and *CZ* are separated the *OLZ*. The *SZ* is found to the S of the *OLZ* and represents a thick sequence of metaturbidites, forming a SE-verging thrust belt, characterized by high-P low-T metamorphic conditions (*Stanistreet et. al., 1991; Kukla et al. 1991*).

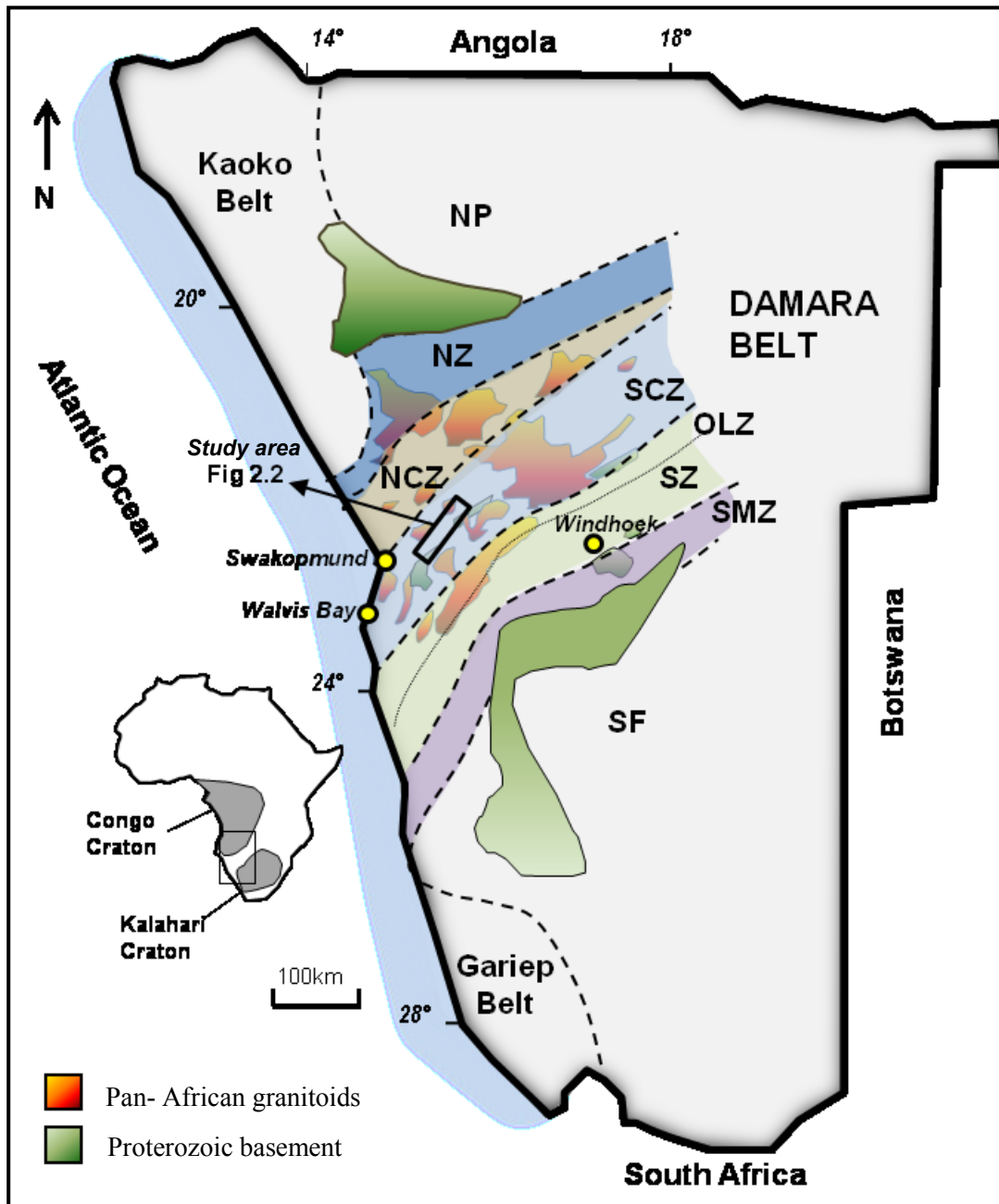


Figure 2.1, Tectonostratigraphic map of the Damara Orogen in Central Namibia (after Miller, 1983, modified from Kitt, 2008). *NP*: Northern Platform; *NZ*: Northern Zone; *NCZ*: Northern CZ; *SCZ*: Southern CZ; *OLZ*: Okahandja Lineament Zone; *SZ*: Southern Zone; *SMZ*: Southern Margin Zone; *SF*: Southern Foreland.

### 2.1.2 Tectonostratigraphic Evolution of the CZ in the Damara Belt

The sequence of events leading to the development of the Damara Orogen is subdivided into five main phases. They are 1) rifting, 2) progressive basin evolution and marine sedimentation, 3) convergence, 4) collision, and 5) post-collisional equilibration.

#### 1) Rifting

The creation of Neoproterozoic basins was initiated by rifting along a triple junction between the Kalahari, Congo and Rio de la Plata- Cratons. Rifting was already in progress by ~750Ma as is apparent from U-Pb zircon ages from rhyolitic volcanics ( $746 \pm 2\text{Ma}$ ) and quartz syenite plugs ( $756 \pm 2\text{Ma}$ ) in the sedimentary sequence (Hoffman *et al.*, 1996). In the Damara Belt, the lowermost unit of the Nosib Group, the Etusis Formation, was formed by the deposition of clastic sediments such as arkoses, conglomerates and sandstones, together with volcanic and volcanoclastic rocks into this rift basin (Miller, 1983). The Etusis Formation unconformably overlies the older, Mesoproterozoic basement gneisses of the Congo Craton (Jacob *et al.*, 1983). The Etusis Formation, in turn, is overlain by calc-silicate felses, gneisses, biotite schist, graphite schists and marbles of the Khan Formation (Jacob, 1974; Miller, 1983), deposited in a shallow-marine environment.

#### 2) Progressive basin evolution and marine sedimentation

Continued rifting caused the opening and marine incursions into two major, E- trending basins, namely the N, more restricted Outjo Sea and the southern Khomas Sea between the Congo and the Kalahari Cratons (Stanistreet *et al.*, 1991; Miller, 2008). The deposition of the lower Swakop Group in the CZ is thought to have occurred in a shelf- or continental-slope environment, following thermal subsidence and the major marine transgression (Hartnady *et al.*, 1985; Henry *et al.*, 1988; Stanistreet *et al.*, 1991; Hoffmann, 1990). The Swakop Group is a mixed carbonate siliciclastic succession, also containing two glaciomarine formations related to major and probably global glaciations in the outgoing Neoproterozoic (Hoffmann *et al.*, 2004). From bottom to top, it consists of the Chuos Formation diamictite, the metaturbiditic Spes Bona Formation, the mainly carbonates of the Okawayo Formation, metaturbidites, volcanics and diamictites of the Oberwasser Formation (after Badenhorst, 1992; Oberwasser Member and Ghaub Formation after Hoffman *et al.*, Miller, 2008), thick carbonate successions of the Karibib

Formation and the topmost siliciclastic, metaturbidite- dominated rocks of the Kuiseb Formation. Radiometric ages constraining the timing of this sedimentation are sparse, but Hoffmann et al. (2004) recently obtained a U-Pb zircon age of  $635\pm 2$ Ma from a rhyolitic horizon in the upper parts of the Oberwasser Formation and associated diamictite units.

### 3) Convergence

The onset of crustal convergence and closure of the Khomas Sea is not well constrained, but is generally assumed to have commenced at ca. 600 to 580 Ma (Miller, 1983). In the Damara Belt, convergence can be attributed to the N-ward subduction of the Kalahari Craton underneath the Congo Craton (Miller, 1983). The obliquity of subduction and also later collisional tectonics is controversial and ranges from an oblique, N- to NE-directed subduction (Oliver, 1994; Miller, 2008), to high-angle NW-directed subduction and collision (Stanistreet et al., 1991; Kisters et al., 2004). The SZ of the Damara Belt is interpreted by Kukla et al. (1991) as an accretionary prism, formed during the NW-directed subduction of the Kalahari Craton beneath the Congo Craton (Kasch, 1983). Convergence occurs simultaneously with the generation of the first granitoids. Numerous small gabbroic, dioritic and syenitic plutons intruded throughout the central Damara Belt during this phase of crustal convergence (Jacob et al., 2000; de Kock et al., 2000). Crustal convergence between ca. 580-550Ma was associated with the development of a regional bedding-parallel ( $S_1$ ) fabric, and large-scale thrusting and recumbent folding ( $D_1$ ) (Miller, 1983).

### 4) Collision

Continued convergence eventually led to the collision of the Kalahari and Congo Cratons. This occurred between ca 550 and 540 Ma (Miller, 1983, 2008; Jacob et al., 2000; Kisters et al., 2004; Johnson et al., 2006) but the effects of the collisional event can be recognized to ca. 510 Ma (Jung and Mezger, 2003). The collision is responsible for the dominant ENE-trending structural grain in the CZ of the Damara Belt, refolding earlier  $D_1$  related fabrics and regional scale folds. The regional structural geology within the CZ is discussed by many authors and remains a very contentious topic.

Between two and four, and up to five deformational phases have been proposed by different authors (e.g. Jacob, 1974; Miller, 1983; Kasch, 1983; Coward, 1983; Steven, 1993; Oliver,

1994; Poli and Oliver, 2001; Kisters et al., 2004). The often co-axial nature of the deformation and e.g. refolding of structures seems to provide evidence for a progressive deformation, rather than multiple deformational events.

**D<sub>1</sub>** is convergence-related and responsible for the earliest structures. D<sub>1</sub> manifests itself as bedding parallel foliation (S<sub>1</sub>), intrafolial and regional-scale isoclinal folds and nappes (F<sub>1</sub>) and low-angle mylonites (Kisters et al., 2004).

**D<sub>2</sub>** is regarded as the main deformational event and produced most of the regional-scale structures and is responsible for the bivergent structure of the South CZ. Structures like the SW-trending dome structures and intervening synclines as well as large-scale thrusts and detachments are a result of the D<sub>2</sub> deformation (Figure 2.2). The more recent works by Poli and Oliver (2001) and Kisters et al., (2004) emphasize the role of the lateral extrusion of rocks during the D<sub>2</sub> deformation, relating the formation of large, SW closing sheath folds (Coward, 1983) to the progressive refolding of regional-scale NE- trending D<sub>2</sub> folds during D<sub>2</sub> (D<sub>2</sub> late). This may explain the difference in the use of terminology with regard to D<sub>2</sub> and D<sub>3</sub> related fabrics.

Late-stage transcurrent shearing is reported from ENE- trending lineaments N and S of the CZ (Tack and Bowden, 1999; Stanistreet et al., 1991; Steven, 1993; Basson and Greenway, 2004) variably referred to as D<sub>3</sub>, D<sub>4</sub> or D<sub>5</sub>, but these have not resulted in pervasive fabrics or structures.

### 5. Post-collisional evolution

The post-collisional evolution of the Damara Belt is characterized by a long thermal history from ca. 530 Ma to 460 Ma (Miller, 1983; Jung et al., 2001; Jung and Mezger, 2003). This thermal history has variably been ascribed to decompression and crustal thinning following collision, along with the intrusion of voluminous granites. The thermal peak in the CZ of the Damara Belt was reached well after the main phase of crustal thickening between ca. 535-500 Ma and seems to coincide with these events. This high-T, low-P metamorphism (M<sub>2</sub>) was episodic and resulted in late- to post-tectonic partial melting of parts of the CZ and basement rocks and the late- to post-tectonic emplacement of mainly S-type leucogranites in the CZ and NZ (Jung et al., 2001; Jung and Mezger, 2003). On a regional scale, the highest metamorphic grades are found in the SW of the Damara Belt along the Atlantic seaboard, decreasing towards the NE and further inland. The peak-metamorphic conditions in the CZ show high-grade conditions of 700–750 °C and 5–6 kbar for the SW part of the CZ (Masberg et al., 1992; Jung et al., 1998, 2001; Jung and

Mezger, 2003). These high-grade rocks contain abundant migmatites. Rocks within the Karibib District, in the NE, show lower amphibolite-facies metamorphism with temperatures between 560 and 650° C and pressures of  $3 \pm 1$  kbars (Puhan, 1983; Steven, 1993). Ar-Ar mica ages of ca. 460 Ma indicate the final uplift and cooling of the Damara Belt by mid-Ordovician times (Gray et al., 2006).

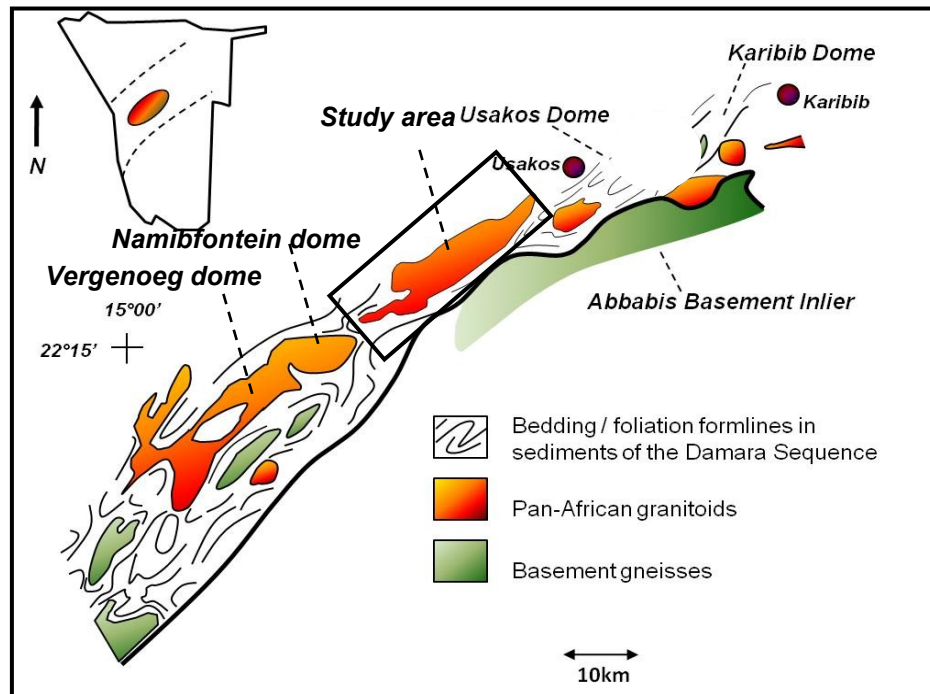


Figure 2.2, Simplified formline map showing the regional-scale NE trending dome structures in the South CZ. Most of the domes are cored by basement gneisses or Pan-African granitoids, with the Damara sequence draped around the domes (after Kisters et. al., 2004, modified from Kitt, 2008)

### 2.1.3 Granite plutonism in the CZ of the Damara Belt

Pan-African granites and related rocks cover an area of over 75000 km<sup>2</sup>, being particularly common in the CZ, the so-called magmatic axis of the belt. Granitoids are overwhelmingly granites (*sensu stricto*), but compositions range from gabbro/diorite to tonalite/granodiorite to granite in proportions of 2:2:96 (*Miller, 1983*).

In the sCZ, granitoids show a clear sequence of intrusion from earlier gabbros via diorites and granodiorites to porphyritic biotite granites and granodiorites to late-stage leucogranites (*Miller, 1983; 2008; Jung et al., 1998*). U-Pb zircon ages indicate an emplacement of the more mafic rock suites between ca. 565 Ma and 555 Ma (*Jacob et al., 2000; Jung et al., 1998*). This corresponds to fabric and wall-rock contact relationships that suggest an emplacement after the D<sub>1</sub> deformation, but pre- or syn- D<sub>2</sub> (D<sub>3</sub>, *after Miller, 1983, 2008*). The voluminous and regionally widespread suite of porphyritic biotite granites mainly encompasses the Salem Granitic Suite, more commonly referred to as Salem-type granites (*Jacob, 1974; Miller, 1983*). The Stinkbank granite investigated in this study forms part of the Salem-type granites (*Marlow, 1983*). Salem-type granites combine a number of characteristic features (*Jacob, 1974; Marlow, 1983; Miller, 1983, 2008; Johnson et al., 2006a*). Salem-type granites in the sCZ typically intrude at the stratigraphic level immediately above the thick marble unit of the Karibib Formation and into the basal parts of the siliciclastic, schist-dominated Kuiseb Formation. Moreover, the granites commonly occupy the cores of regional-scale D<sub>2</sub> (D<sub>3</sub>, *after Miller, 2008*) NE- trending synclinal structures. Commonly depicted as steep-sided, sharply cross-cutting plugs on regional maps (*Smith, 1965*), more recent works suggest rather semiconcordant, sheet-like or lopolithic geometries (*Johnson, 2005; Miller, 2008*). Leucogranites form the last and largely post-tectonic suite of granite plutons in the sCZ. *Jacob et al. (2000)* reported U-Pb zircon ages of 539 ± 6 Ma for the post-D<sub>2</sub> Rote Kuppe Granite, outside Karibib. Post-tectonic granite plutonism is recorded in the sCZ until ca. 460 Ma, including the uraniferous leucogranites, locally referred to as alaskites, of the SW parts of the sCZ around Goanikontes and the Rössing mine (*Tack and Bowden, 1999; Jung and Mezger, 2001, 2003; Basson and Greenway, 2004*).

## 2.2 The Stinkbank granite- previous work

The Stinkbank granite intrudes into the SW extent of the Kransberg Syncline, bordered in the S by Abbabis basement and the SW termination is marked by Namibfontein and Vergenoeg domes (Figure 2.2) (Smith, 1965; Kröner, 1984; Poli and Oliver, 2001). The granite is mainly hosted by schists of the Kuiseb Formation and above marble units of the Karibib Formation, corresponding to Miller's (1983) general assertion that Salem-type granitoids are preferably emplaced in synformal structures and in the lower parts of the Kuiseb Formation.

Covering an area of 600km<sup>2</sup>, with an elongate shape, tapering to the SW, Marlow (1983) was the first worker to study the Stinkbank granite in detail. He distinguished an earlier porphyritic, biotite-rich phase from a later, porphyritic and leucocratic phase, which is the typical association of granite phases found in Salem-type granites (e.g. Jacob, 1974; Miller, 1978). Marlow (1983) also describes NE trending magmatic and solid state fabrics which he ascribed to the largely syn-tectonic (D<sub>2</sub>) emplacement of the pluton. Miller (2008), in turn, described the leucocratic phase of the Stinkbank granite as being post-tectonic. A very imprecise Rb-Sr isochron age of 601 ±79 Ma was considered to be geologically not relevant by Marlow (1983). U-Pb zircon ages from the NE extremities of the Stinkbank granite suggest an emplacement age of 549 ± 11 Ma (Johnson et al., 2006 a), corresponding to a largely syn-D<sub>2</sub> timing of emplacement.

### **3. LITHOSTRATIGRAPHY AND FIELD RELATIONS**

#### ***3.1 Introduction***

The Stinkbank granite is intrusive into and almost exclusively in contact with rocks of the Kuiseb Formation of the Damara Supergroup (Table 3.1). Johnson (2005) also describes intrusive relationships with the marble-dominated units of the Karibib Formation to the NW of the present study area. The lithostratigraphic subdivision of the Damara Supergroup adopted here follows that of Badenhorst (1992), who established the lithostratigraphy and correlations of formations for this part of the sCZ (Table 3.1). Importantly, the central, schist- and marble-dominated formations of the lower Swakop Group (Table 3.1) are largely absent from the study area and only found in the far SW closure of the Kransberg syncline. These formations will not be discussed, but are mentioned in Chapter 3.2.2. In addition, the Rössing- and Khan Formations of the underlying Nosib Group and lower most Swakop Group are only developed to the SW of the study area and will only be discussed briefly (Chapter 4). Formations developed in the study area include, from bottom to top, the Etusis-, Karibib- and Kuiseb Formations (Table 3.1). These formations are exposed on the limbs of the Kransberg syncline, the youngest Kuiseb Formation also occupies much of the core of the syncline to the NE and between the towns of Karibib and Usakos. In the study area and to the SW of Usakos, the Kransberg syncline is intruded by granite phases related to the Stinkbank granite, that occupy the core of the first-order fold structure. Rocks of the Kuiseb Formation occur as variably sized (decimetres- to several hundred meters in length and width) xenoliths within the granite. Throughout the study area, the Kuiseb Formation is structurally underlain and rimmed by marbles of the Karibib Formation, underlining the synclinal nature of the Kransberg syncline. The arkoses and quartzites of the Etusis Formation underlie the Karibib Formation in the SE, bounded by basement rocks of the Abbabis Metamorphic Complex.

*Lithological map*

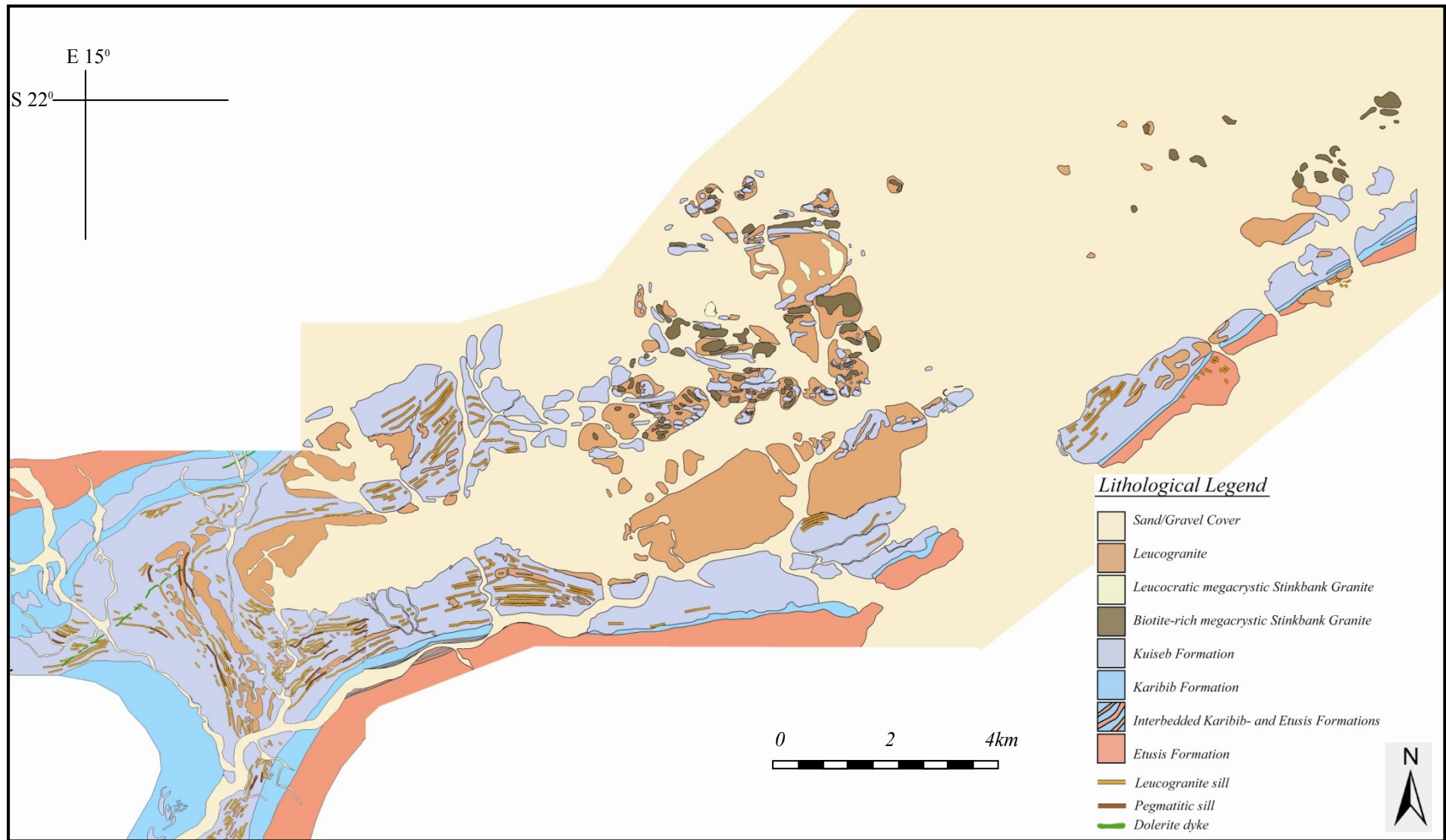


Figure 3.1, Geological map of the study area showing the main lithological units exposed within the Kransberg syncline

Table 3.1, Stratigraphy of the Damara Sequence. Formations developed in the study area are highlighted in bold (modified from Badenhorst, 1992, Kitt 2008 and Miller 2008 ).

<u>Damara Sequence</u>	<u>Group</u>	<u>Formation</u>	<u>Lithologies</u>
	<u>Swakop Group</u>	<b>Kuiseb</b>	
<b>Karibib</b>			<i>Bluish-grey calcitic marbles, beige to bright white dolomitic marbles and banded calc-silicate felses of a reddish brown colour. Thin horizons of cordierite- biotite schists also occur.</i>
Oberwasser			<i>Dark grey biotite and biotite cordierite schists, calc-silicate felses, minor carbonate breccia horizons, including glaciomarine pelites and dropstone units of the Ghaup Formation and interbedded amphibolites of the Daheim Member in the upper parts of the unit.</i>
Okawayo			<i>Calcitic and dolomitic marbles and intercalated calc-silicate felses, locally intruded by mafic sills and dykes.</i>
Spes Bona			<i>Dark grey biotite and biotite-cordierite schists, calc-silicate felses with minor amphibolites, metapsammites and marbles.</i>
Chuosi			<i>Glaciomarine diamictite</i>
Rössing			<i>Interbedded marbles, calc-silicates and siliclastic rocks.</i>
<u>Nosib Group</u>		Khan	
	<b>Etusis</b>		<i>Well bedded reddish-pink feldspathic quartzites. Arkoses, conglomerates and minor metavolcanics.</i>
<b><u>Ababis Basement</u></b>			<i>Pink and grey quartzo-feldspathic augengneisses, schists, amphibolites and pegmatites</i>

### ***3.2 Pre-Damaran Basement***

- *Abbabis Metamorphic Complex*

The Abbabis Metamorphic Complex is made up of mainly quartzofeldspathic gneisses. These gneisses consist of an assortment of pink and grey quartzofeldspathic augen gneiss as the main rock type, red muscovite-rich quartzite with conglomerate layers in places, and plagioclase-rich biotite gneiss, as described by Smith (1965).

In the field, these basement rocks can be found juxtaposed against quartzites of the Etusis Formation. Although the rocks of the Etusis show very steep- to overturned dips, the basement gneisses show shallow dips towards the SW, indicating the angular unconformity between the basement and the overlying Damara Supergroup (see Chapter 4).

### ***3.3 The Damara Sequence***

#### ***3.3.1 Rocks of the Nosib Group***

- *Etusis Formation*

The Etusis Formation forms the lowermost formation of the Damara Supergroup, forming part of the Nosib Group, the continental, rift-type succession of the Damara Belt (Miller 1983). The rocks of the Etusis Formation are exposed along the southern limb of the Kransberg syncline (Figure 3.2, a). In the field area, the formation consists of arkosic metasediments and thin, interbedded metapelitic and metaconglomeratic units. The arkoses still preserve massive bedding and cross bedding (Figure 3.2, b). The preservation of primary sedimentary features implies that the rocks show much lower strain intensities compared to the overlying Karibib- and Kuiseb Formations.

Rocks have a distinct reddish brown colour and are found in contact with marbles of the Karibib Formation in the north, and the Abbabis Metamorphic Complex to the S. The thickness of the formation varies between 100 and 500m in the field area. Bedding within the Etusis Formation is steep to subvertical, with a dip direction towards the NW and SE. Contacts between the Etusis Formation and marbles of the overlying Karibib Formation are very sharp and easily followed. The Khan Formation is only developed in the adjacent Namibfontein/ Vergenoegd domes to the SW of the study area (Poli and Oliver, 2001).

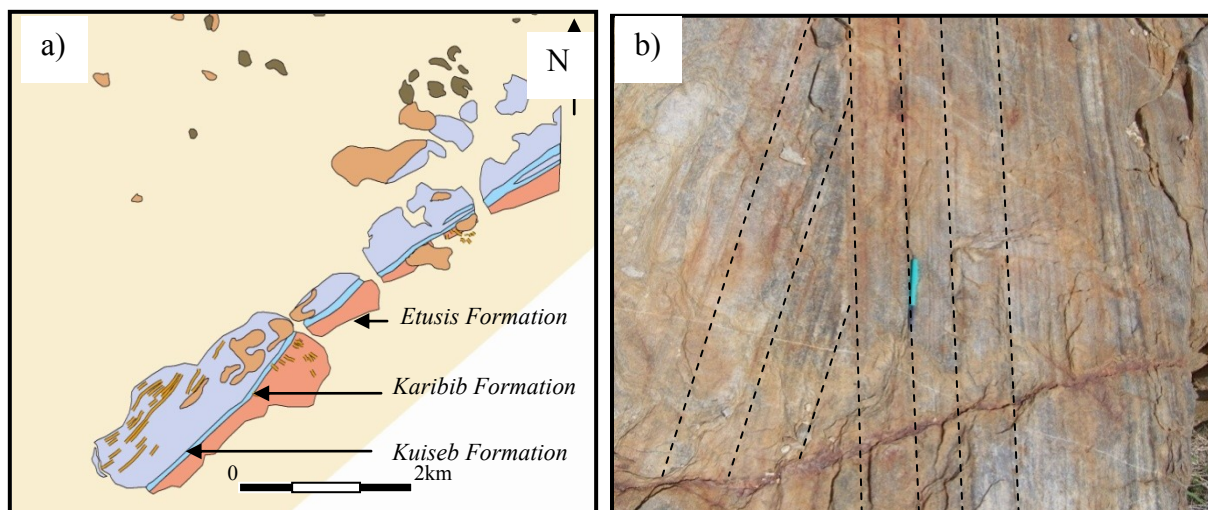


Figure 3.2, a) Map insert, taken from the lithological map. Three formations delineated along the S-limb of the Kransberg synform. The Etusis Formation, Karibib Formation and Kuiseb Formation are all exposed along the S- limb.

b) Arkoses of the Etusis Formation with prominent cross bedding, annotated.

### 3.3.2 Swakop Group

The lower formations of the Swakop Group, including the Rössing-, Chuos-, Spes Bona-, Okawayo- and Oberwasser Formations are not developed in the study area and will not be discussed.

#### *3.3.2.1 Karibib Formation*

The Karibib Formation represents a thick marble-dominated unit. This unit contains mainly bluish-grey calcitic marbles, beige- to bright-white dolomitic marbles and banded calc-silicate felses of a reddish-brown colour (Figure 3.3, a, b). Thin horizons of cordierite- biotite schist also occur. Rocks of the Karibib Formation are mainly exposed along the southern limb of the Kransberg syncline, where they are found as a thin (20 – 100m), highly recrystallized horizons between the Etusis and the Kuiseb Formations.

Close to the SW closure of the Kransberg syncline ( $22^{\circ}11'58.30''S$ ;  $15^{\circ}20'34.07''E$ ) the pink and grey marbles of the Karibib Formation are interleaved with arkoses and quartzites of the Etusis Formation (Chapter 4) over an up to 300m wide zone (Figure 3.3, c).

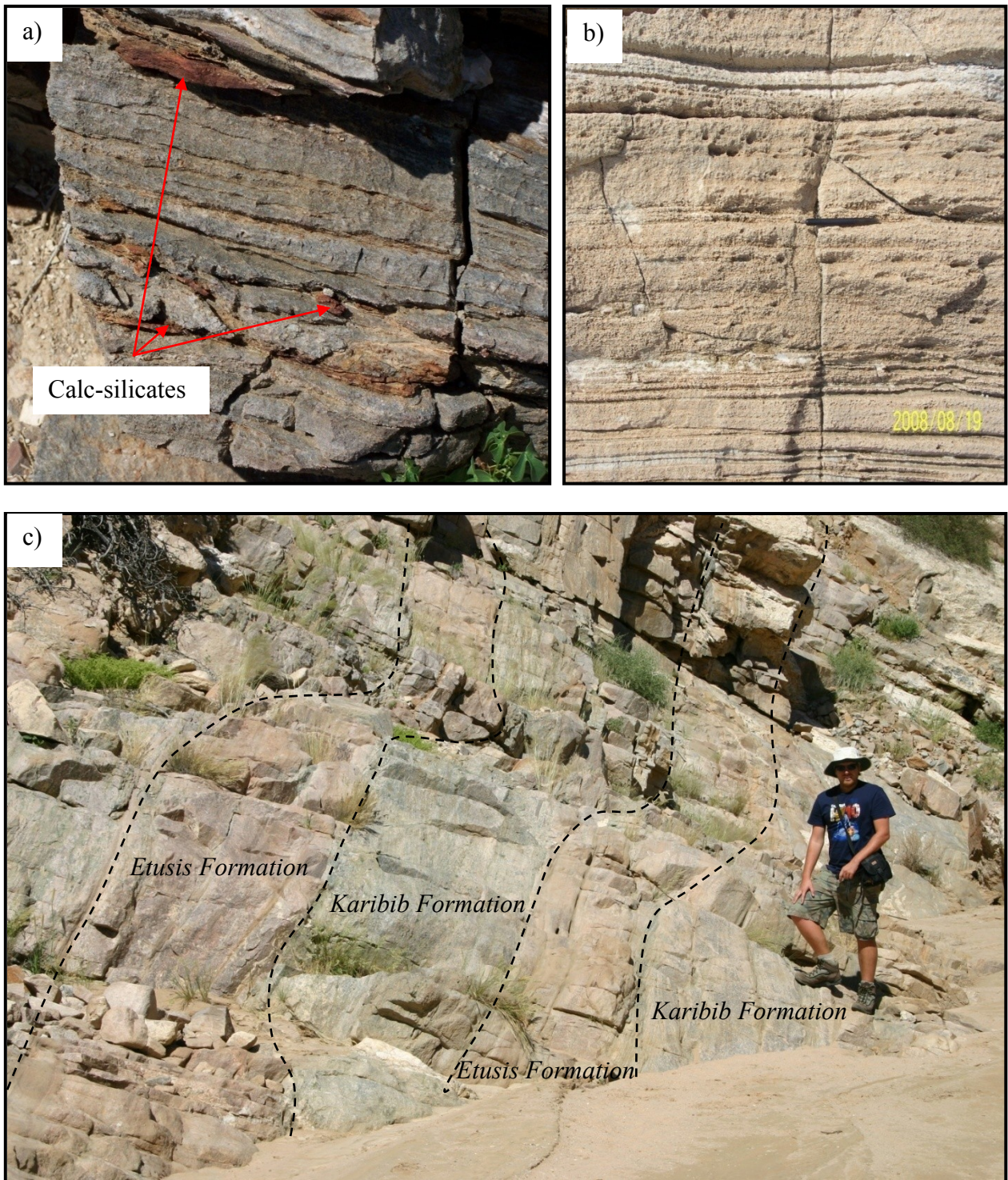


Figure 3.3, a) Weathered calcitic marble (dark grey) with cm-wide, interlayered reddish calc- silicate felses. b) Pink, coarsely recrystallized dolomitic marble that characterizes the Karibib Formation in the field area. Primary sedimentary features are largely obliterated. c) Interbedding between rocks of the Karibib Formation and the Etusis Formation. Khan River, SW of study area.

### 3.3.2.2 Kuiseb Formation

Rocks of the Kuiseb Formation are exposed throughout the entire field area, but are most prominent along the southern limb and in the SW closure of the Kransberg syncline. The Kuiseb Formation is dominated by dark-brown biotite-quartz schists (Figure 3.4, a), interbedded with volumetrically minor calc-silicate felses, marbles and metapsammities and very subordinate marble horizons. The biotite-rich schist units commonly contain cordierite porphyroblasts that can reach up to 1 cm in diameter, giving the schist a spotted appearance (Figure 3.4, b). Within the schists, the preferred alignment of muscovite and biotite defines the schistosity. The metapsammitic units rarely exceed 1m in thickness, but form good, positively weathering marker horizons in the field. Calc-silicate felses are common, but commonly thin (<50cm) and interbedded with the schist units. Internal bedding features such as mm-thick laminations and cross-bedding are locally preserved, particularly in metapsammities, but, for the most part, pervasive foliation development and recrystallization has obliterated fine-scale primary features.

Two main marble horizons are recognized close to the contact with the structurally underlying Karibib Formation. These marble horizons provide excellent marker horizons and can be followed along most of the S- limb of the Kransberg syncline. The true thickness of the Kuiseb Formation cannot be determined since it is the uppermost formation recognized in the Damara Supergroup. Moreover, thickness estimates in the field are complicated by pervasive bedding transposition and structural duplication that has affected the schists (Chapter 4). On a regional scale and in lower strain areas of the south CZ of the Damara Belt, thickness estimates are > 1000m (*e.g. Miller, 1983, 2008*).

Rocks of the Kuiseb Formation are also found throughout the Stinkbank granite, forming clusters of xenoliths or occurring as large rafts, particularly close to the granite wall-rock contacts. These occurrences will be described in detail in Chapter 5.

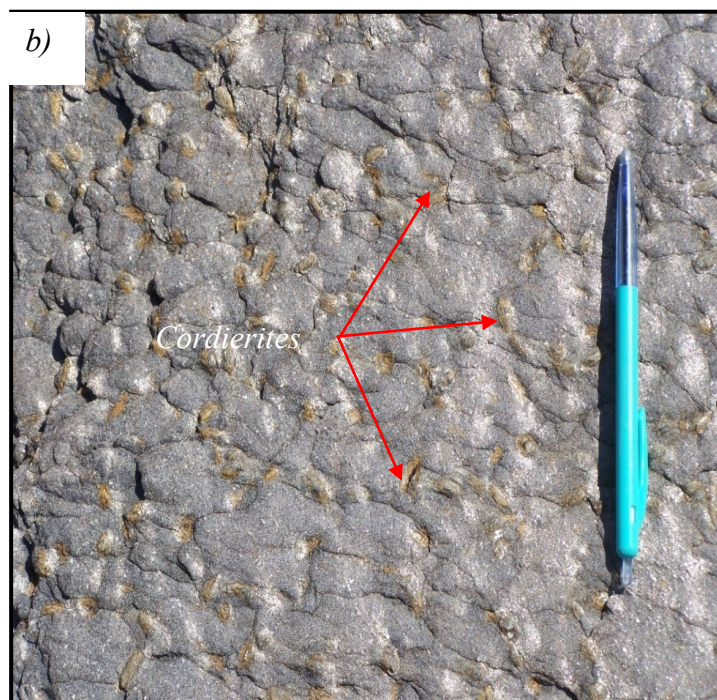
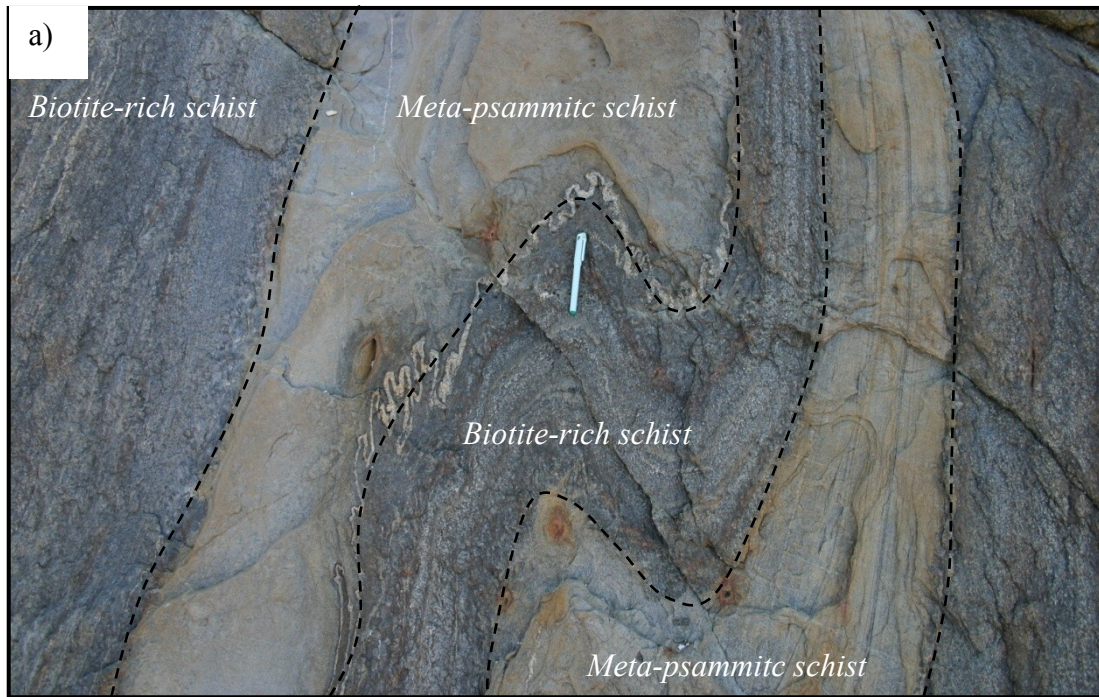


*Figure 3.4 a)* Plan view of interbedded and folded coarse grained biotite- and meta-psammitic schist. The latter generally is lighter in colour and contains no cordierite porphyroblasts.

*b)* Plan view of biotite-quartz schist with cordierite porphyroblasts. The red arrows indicate the cordierites. Regionally these cordierites are aligned and define a lineation ( $L_1$ ).

### 3.3.3 Petrography

The schists of the Kuiseb Formation consist of biotite (50%), quartz, k-feldspar, cordierite and accessory zircon and muscovite. Biotite has a very distinct deep-red colour and shows a strong alignment of its basal planes (Figure 3.5 a, b). In places, biotite contains small zircons identified by the dark, heterokinetic halos around them (Figure 3.7). Cordierite is commonly weathered, and partial to complete pinitization of cordierite is widespread (Figure 3.8). Quartz in the matrix is fine grained and forms statically recrystallized textures with straight quartz grain boundaries and  $120^{\circ}$  triple point junctions between the grains (Figure 3.9).

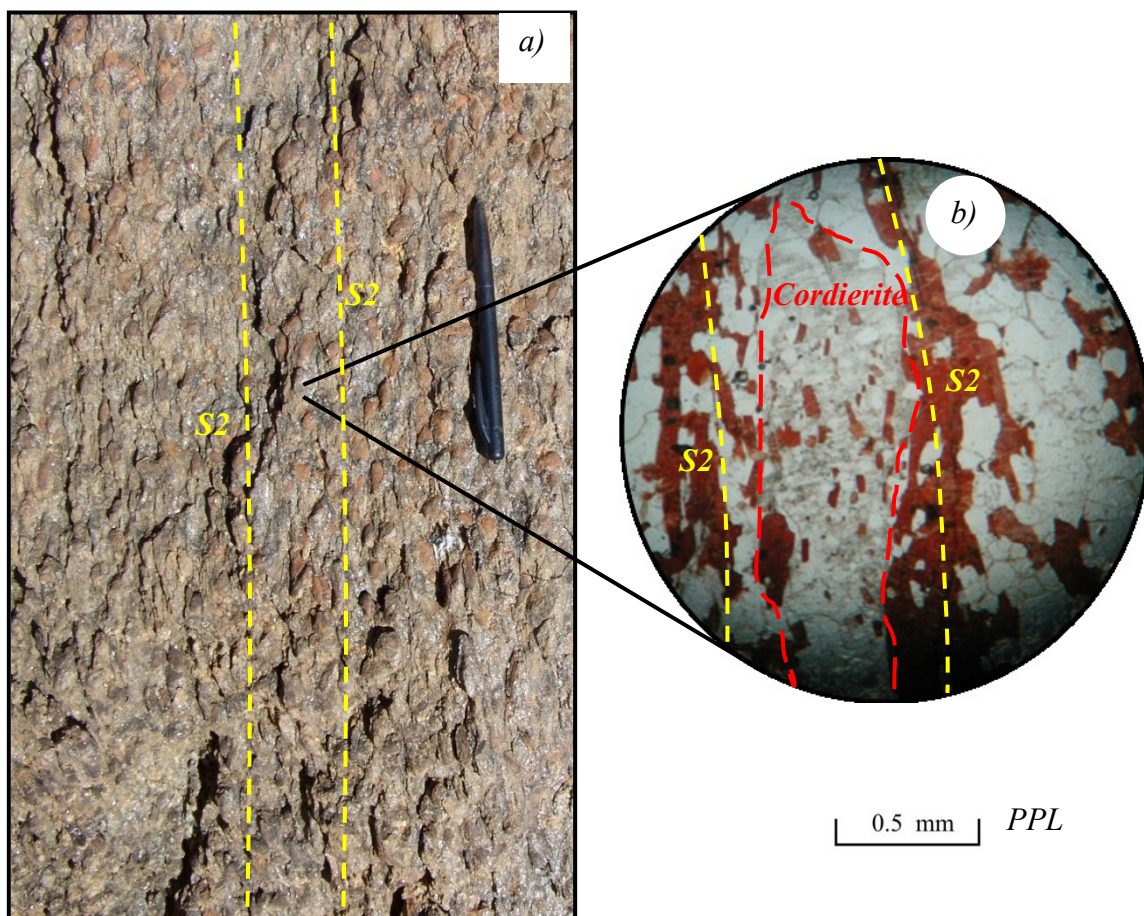


Figure 3.5 a, Plan view of cordierite-rich biotite schist of the Kuiseb Formation. b) Biotite-cordierite schist of the Kuiseb Formation in thin section, showing a flattened cordierite (annotated) enveloped by a schistosity defined by biotite and quartz (-feldspar) ribbons. Plain polarized light.

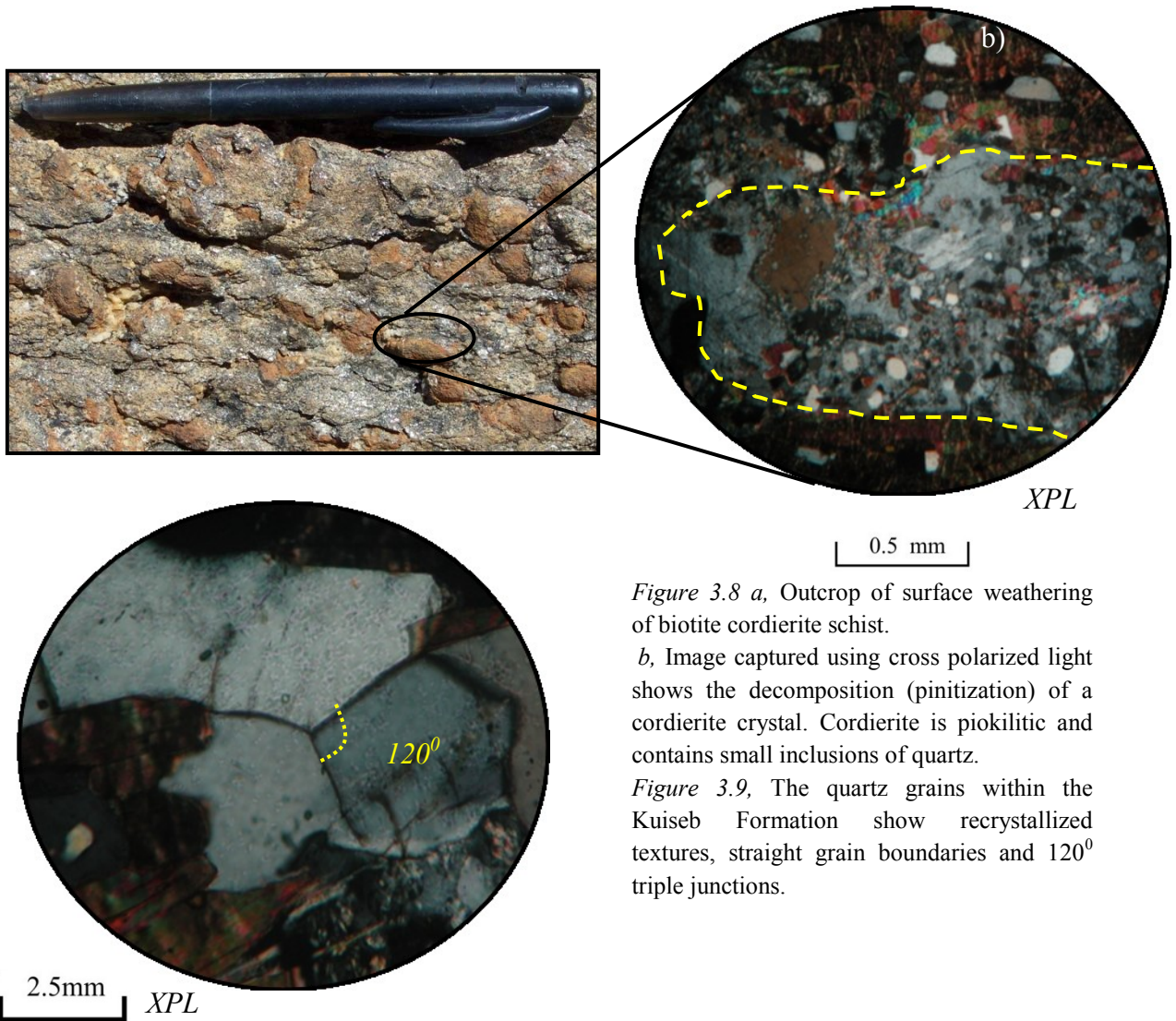


Figure 3.8 a, Outcrop of surface weathering of biotite cordierite schist.

b, Image captured using cross polarized light shows the decomposition (pinitization) of a cordierite crystal. Cordierite is piokilitic and contains small inclusions of quartz.

Figure 3.9, The quartz grains within the Kuiseb Formation show recrystallized textures, straight grain boundaries and  $120^\circ$  triple junctions.

### 3.4 Intrusive Rocks

#### 3.4.1 Granitic and pegmatitic sills and dykes intrusions

The distribution of the granite is shown in Appendix 1, Geological map. A detailed discussion of these granites and pegmatite sills will be done in Chapter 5.

#### 3.4.2 Dolerite dykes

The study area contains only a singular dolerite dyke. It crosscuts beds of the Kuiseb Formation near the SW closure of the Kransberg synform ( $22^\circ 11' 0.54''\text{S}$ ;  $15^\circ 18' 43.54''\text{E}$ ). Weathering causes the dyke to present itself as a distinct black ridge. They can also be identified by the characteristic onion skin weathering. Dolerite dykes are generally of Karoo age in central Namibia.

## **4. STRUCTURAL GEOLOGY**

### **4.1 Introduction**

Based on relative age and cross cutting relationships between fabrics, two main phases of deformation,  $D_1$  and  $D_2$ , can be identified in the study area. This agrees with the findings of earlier works done by Poli and Oliver (2001) and Johnson (2005) in adjoining areas to the SW and E.

Structural elements are summarized in Table 4.1

Conventions used are as follows:

- S, planar fabrics
- L, linear fabrics
- F, folding of planar and linear fabric
- 1, 2 refer to deformational phase  $D_1$  and  $D_2$  respectively.

The following chapters provide a brief outline of the structural geology of the wall rocks of the Stinkbank granite, before which the actual emplacement and emplacement controls of the granite can be discussed.

Table 4.1, Summary of the main fabric and structural elements observed within the study area.

<u>Deformational Phase</u>	<u>Strain Regime</u>	<u>Fabric Element</u>	<u>Fabrics</u>
			<u>Field expression, and occurrence of fabric</u>
<u>Primary</u>		S <sub>0</sub>	Primary compositional layering (Bedding). Cross bedding within quartzites of the Etusis Formation.
<u>D<sub>1</sub></u>	Low angle shearing	S <sub>1</sub>	Bedding-parallel schistosity within metapelitic units. Defined by the orientation of biotite within the Kuiseb Formation.
		F <sub>1</sub>	Intrafolial folds, bedding transposition within the Kuiseb Formation
<u>D<sub>2</sub></u>	NW-SE directed shortening. Collision of the Kalahari- and Congo cratons (ca. 550 -530 Ma)	S <sub>2</sub>	Axial planar foliation
		F <sub>2a</sub>	1 <sup>st</sup> Order Kransberg Syncline, kilometre scale synclinal structure
		F <sub>2b</sub>	2 <sup>nd</sup> order fold structures. Exposed as antiforms and synforms within the larger Kransberg Syncline. Half wavelengths between 50m and 500m
		F <sub>2c</sub>	Parasitic, lower order folds to the F <sub>2b</sub> folds. Half wavelengths range between 5 and 50 m.
		F <sub>2d</sub>	Parasitic, lower order folds to the F <sub>2c</sub> folds, Half wavelengths range between a few centimetres and 5m's
		L <sub>2a</sub>	Mineral preferred orientation. For example the alignment of cordierite within units of the Kuiseb Formation.
		L <sub>2b</sub>	Plunges of lower order folds, F <sub>2c</sub> and F <sub>2d</sub> . Variable throughout the study area.

## 4.2 Primary Bedding ( $S_0$ )

Primary bedding can be identified by lithological variations within the different formations of the Damara Supergroup. Along the southern limb of the Kransberg syncline, lithologies trend NE– SW, dipping at between 75 and 90 degrees towards the NW and SE. However, isoclinal folds ( $F_1$  and  $F_2$ ) testify to some degree of bedding transposition so that the thickness of units cannot be regarded as the true stratigraphic thickness. Within the Kuiseb Formation, calc-silicate felses and isolated marble horizons form relatively good marker horizons in the otherwise compositionally homogeneous sequence dominated by biotite- (cordierite) schists (Figure 4.1). Marbles of the Karibib Formation have a very characteristic white-bluish or pink colour. They are recrystallized and banded, but the banding is probably not primary. In the far SW of the study area, the marbles are interlayered with rocks of the Etusis Formation, suggesting a tectonic imbrication and structural nature of this contact (Chapter 4.5). The Etusis Formation preserves primary features such as cross-bedding and planar bedding, indicating lower strain intensities. The basement consists of gneisses, schists and amphibolites. Basement gneisses are unconformably overlain by the Etusis Formation exposed at e.g. coordinates (22° 9'38.16"S; 15°27'45.56"E, Appendix 1) where shallow SW dipping basement is overlain by steep NW and SE dipping rocks of the Etusis Formation.

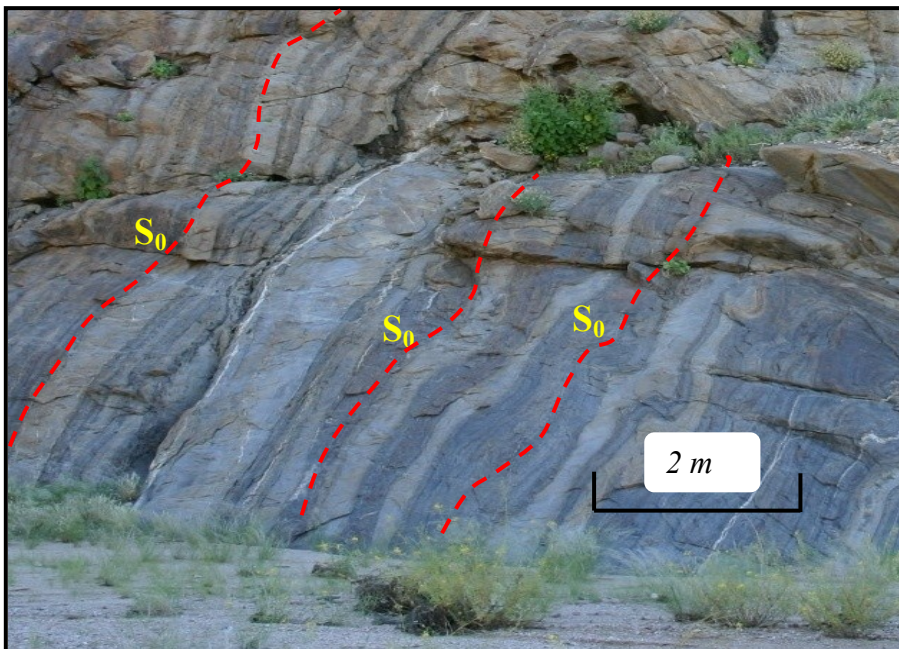


Figure 4.1, Oblique view of the Kuiseb Formation, showing well-preserved bedding ( $S_0$ ). It also shows the internal heterogeneity of the formation, containing lighter metapsammitic units and darker biotite-cordierite schists.

### **4.3 Tectonic Fabrics**

#### *4.3.1 Foliation ( $S_1$ )*

This fabric is particularly recognised within metapelitic units such as the Kuiseb Formation. It is defined by the preferred orientation of bedding-parallel micas, mainly biotite and minor muscovite (Figure 3.8 a, b). The bedding-parallel  $S_1$  foliation is most readily distinguished from the later  $S_2$  fabric in the hinge zones of  $F_2$  folds, including the first-order Kransberg syncline as well as parasitic  $F_{2c, d}$  folds (see below), as  $S_1$  is refolded by  $F_2$  folds and crosscut by the  $S_2$  foliation, which is axial planar to  $F_2$  folds.  $S_1$  seems largely absent from the massive arkoses of the Etusis Formation. Marble units of the Karibib Formation on the SE limb of the Kransberg syncline are strongly foliated, but this fabric is largely ascribed to  $S_2$  (see below).

#### *4.3.2 Foliation ( $S_2$ )*

$S_2$  is an axial planar foliation to  $F_2$  folds. It is defined by a strong preferred orientation of biotite, muscovite or flattened quartz grains and pressure solution seams (Figure 4.2, a) in metapelitic units of the Kuiseb Formation. It commonly shows NE trends and steep dips, mainly to the SE, indicating the NW vergence of the Kransberg Synform and  $F_2$  folds, in general. The  $S_2$  foliation crosscuts the  $S_1$  foliation within the hinge zones of  $F_2$  folds, where the two foliations are at approximately right angles to each other (Figure 4.2, b). This foliation can also be seen within the Salem-type Stinkbank granite. Here the foliation is defined by the alignment of quartz- ribbons (solid-state fabric) and K-feldspar megacrysts and biotite (magmatic fabric, Chapter 5).

#### *4.3.3 Lineations ( $L_{2a}$ )*

Stretching lineations ( $L_{2a}$ ) are defined by the preferred orientation of rod-shaped, stretched cordierite nodules, quartz-feldspar and quartz aggregates (Figure 4.2, c). These are especially noticeable within units of the Kuiseb Formation that contains abundant cordierite.  $L_{2a}$  lineations plunge mainly to the NE and SW, parallel to  $F_2$  folds. Rodding fabrics and constrictional-type strains become prominent in the SW termination of the Stinkbank granite, where rocks of the Damara Supergroup are folded into two funnel-shaped synforms, defining cleavage triple-points related to fold interference (Chapter 4.6). Other lineations include e.g. the orientation of boudin long axes and fold hinges ( $L_{2b}$ , Figure 4.2, a).

## 4.4 Folding

### 4.4.1 $F_1$ folding

An early  $F_1$  fold generation is related to the  $D_1$  deformational event. These folds are typically tight to isoclinal, intrafolial ( $S_1$ ) folds that have refolded bedding,  $S_0$  (Figure 4.2, d). These folds can be seen within schists of the Kuiseb Formation and are also suspected in the Karibib Formation, although pervasive recrystallization of the marbles and later  $D_2$  strains have largely obliterated any earlier primary and structural features in the marbles. The massive arkoses and quartzites of the Etusis Formation have largely retained primary features such as planar and cross-bedding, indicating their competence relative to the schist and marble units.

### 4.4.2 $F_2$ folding

$F_2$  folds are the most common folds in the study area. The NE trending folds are characteristic for the CZ of the Damara Belt and are related to the  $D_2$  deformation event (*Jacob, 1974; Poli and Oliver, 2001; Kisters et. al., 2004;* but  $D_3$  after *Miller, 1983*).  $F_2$  folds are subdivided into four subgroups,  $F_{2a}$ ,  $F_{2b}$ ,  $F_{2c}$  and  $F_{2d}$ , depending on the size of folding, representing first- to lower order folds in the area.  $F_2$ -folding refolds the original bedding,  $S_0$ , and the bedding parallel foliation,  $S_1$ . In the study area, early- $F_2$  folds are NW-verging to upright folds and generally doubly plunging. Plunges of these folds generally range from very shallow up to subvertical and are referred to as  $L_{2b}$  (Figure 4.2, a, d).

$F_{2a}$  folding is represented by the first-order fold of the Kransberg syncline. The syncline is asymmetric, consisting of a steep- to overturned S- limb and a shallowly SE dipping N- limb, resulting in the overall NW- vergence of the fold. The Kransberg synform has a half wavelength of ca. 5km.  $F_{2b}$  and  $c$  folding represent folds with decreasing size and wavelengths.  $F_{2b}$  is parasitic to  $F_{2a}$  and  $F_{2c}$ , in turn, is parasitic to  $F_{2b}$ .

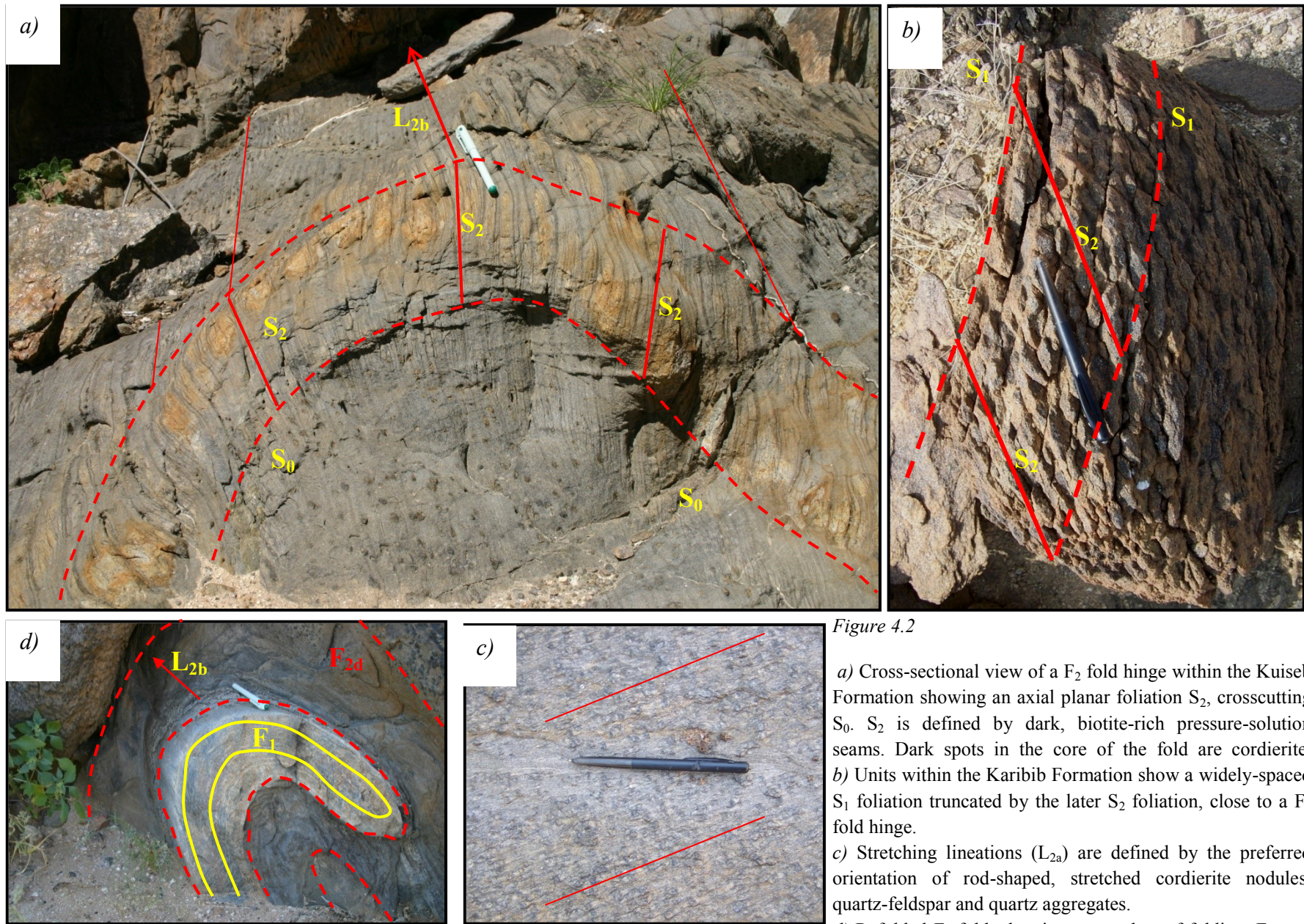


Figure 4.2

a) Cross-sectional view of a  $F_2$  fold hinge within the Kuiseb Formation showing an axial planar foliation  $S_2$ , crosscutting  $S_0$ .  $S_2$  is defined by dark, biotite-rich pressure-solution seams. Dark spots in the core of the fold are cordierite.

b) Units within the Karibib Formation show a widely-spaced  $S_1$  foliation truncated by the later  $S_2$  foliation, close to a  $F_2$  fold hinge.

c) Stretching lineations ( $L_{2a}$ ) are defined by the preferred orientation of rod-shaped, stretched cordierite nodules, quartz-feldspar and quartz aggregates.

d) Refolded  $F_1$  fold, showing two orders of folding,  $F_1$ , and the latter  $F_{2b}$  that refolds  $F_1$ .

#### 4.5. Structural domains

The structural and lithological complexity of the study area and distribution of granite phases with respect to wall rocks requires a subdivision of the study area into smaller domains. Three domains have been selected, based on their structural complexity, variations in the trend of the main structural elements (e.g.  $S_0$ ,  $F_2$  folds), granite/wall rock relationships and lithological variations. The domains 1, 2 and 3 correspond to the SE limb of the Kransberg Syncline (domain 1), including rocks of the Kuiseb-, Karibib- and Etusis Formations and the Abbabis Metamorphic Complex to the SE. The SW closure of the Kransberg Syncline forms domain 2, whereas the central part of the Kransberg Syncline (domain 3) is mainly occupied by the Stinkbank granite (Chapter 5).

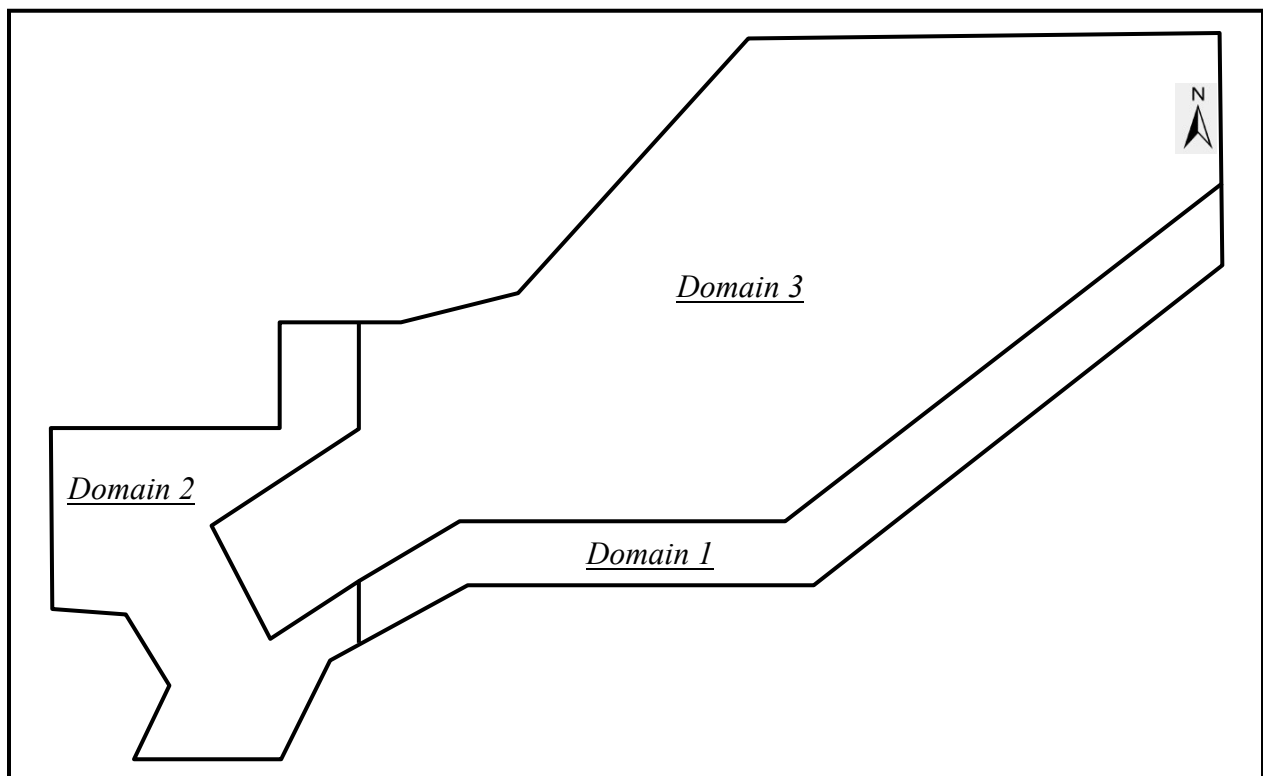


Figure 4.3, Outline of the study area showing the extent and boundaries of domains 1, 2 and 3. Domains 1 and 2 will be discussed in the present chapter. Domain 1 is discussed in Chapter 5, as it is structurally and lithologically distinct from the other two domains, being made up of granite phases of the Stinkbank granite.

## ***4.5 Domain 1***

### ***4.5.1 Wall-rock Structure***

Domain 1 encompasses the S- limb of the Kransberg Syncline (Figure 4.4). The domain is approximately 15km long and traces the S- limb all the way to domain 2, where the bedding of the limb rotates around the SW termination of the Stinkbank granite and into the closure of the Kransberg syncline. The Kuiseb Formation provides the best marker horizon along the S- limb and colour and textural variations between the metapsammitic- and cordierite-bearing schist are easily followed in the field.

On a regional scale, bedding and the  $S_1$  and  $S_2$  foliations in domain 1 are, for the most part, parallel to each other, dipping steeply to the NW or SE, forming the steep- to overturned SE limb of the Kransberg syncline (Figure 4.5, 4.6, 4.7 and 4.8). The parallelism between bedding and the  $S_1$  and  $S_2$  foliation is due to the tight- to isoclinal  $F_1/F_2$  folding that has resulted in intense fabric transposition in large parts of domain 1. Duplication of strata due to refolding of bedding has also resulted in the structural thickening of the Kuiseb Formation, making the determination of the true thickness impossible. Bedding transposition is pervasive between coordinates 22°10'41.11"S; 15°21'58.46"E and 22°10'25.35"S; 15°24'52.78"E (Appendix 1) and original bedding is difficult to identify ("contorted zone" in Figure 4.9 and 4.10). This zone corresponds to an area where granite dykes and sills that are otherwise abundant in the wall rocks are almost completely absent. However, the degree of fabric transposition and fabric intensity decreases from SE to NW and towards the contact between the Stinkbank granite and the Kuiseb Formation. In the SW of domain 1, this contact shows the development of at least one large (halfwavelength ca. 200m), open- to close, shallow doubly-plunging, NE trending  $F_2$  synform. This synform can be traced into domain 2 where it forms a geometrically complex triple junction of three converging synformal structures. Poli and Oliver (2001) have mapped in the adjacent Namibfontein dome and describe these bedding/foliation triple junctions as convergence points, forming as the result of fold interference between adjacent antiformal structures.

**Domain 1**

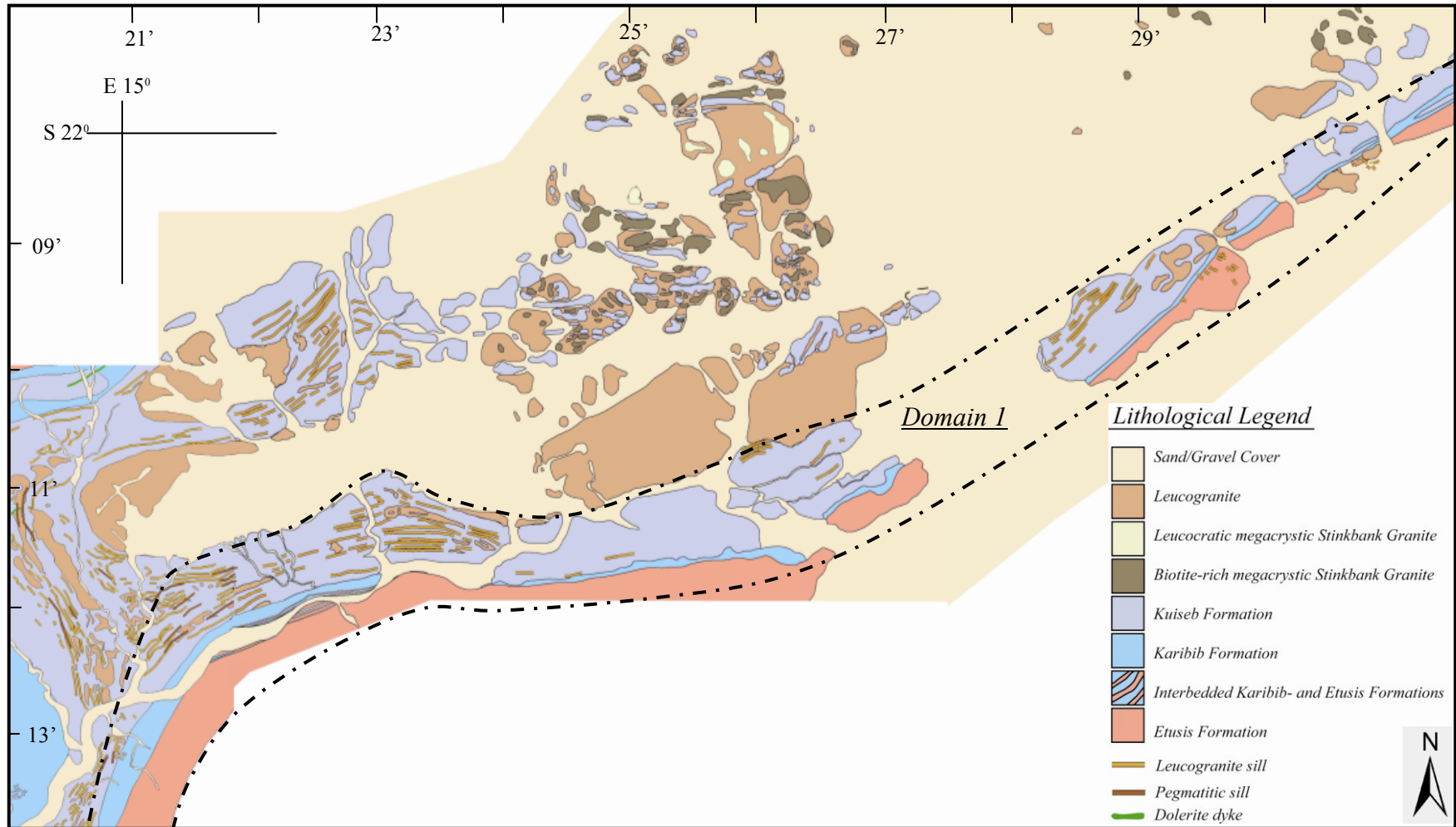


Figure 4.4, Outline of domain 1, covering the S-limb of the Kransberg Syncline, adjacent to the Stinkbank granite, showing a strike extent of over 10km's.

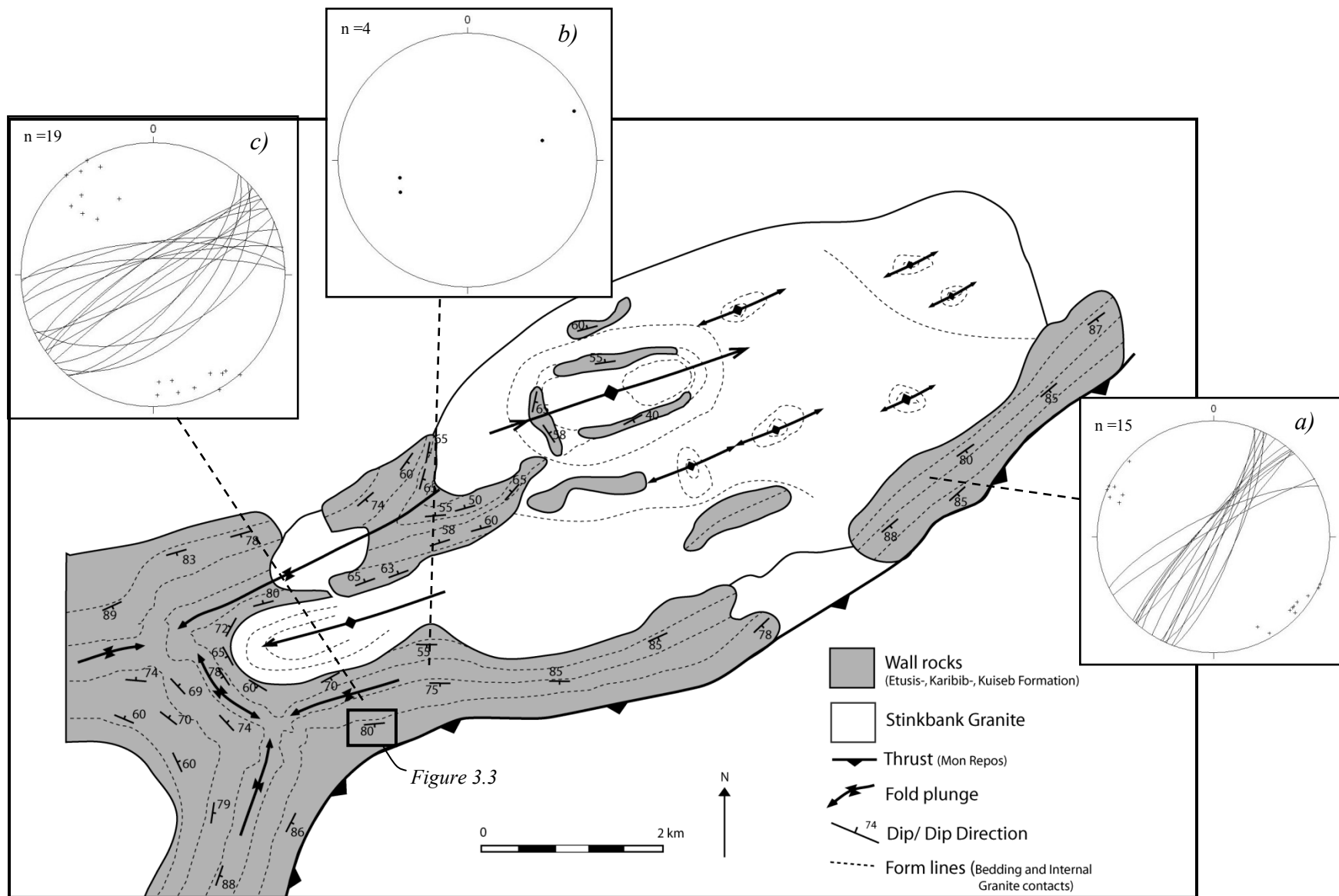


Figure 4.5. Structural formline map of domains 1 and 2. a) Stereonet showing great circles and poles to planes illustrating the steeply dipping and overturned nature of the S- limb of the Kransberg syncline. b) shows the plunge of four large F<sub>2</sub> folds, found within the southern limb of domain 1, close to the SW closure of the Kransberg syncline; c) great circles and poles to planes (S<sub>0</sub>/S<sub>1</sub>) showing the overturned and steeply dipping nature of the S- limb of the Kransberg syncline in the SW parts of domain 1.

*Cross sections of Domain 1*

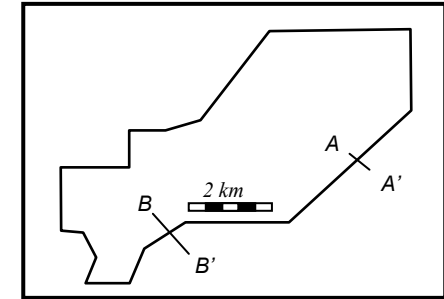
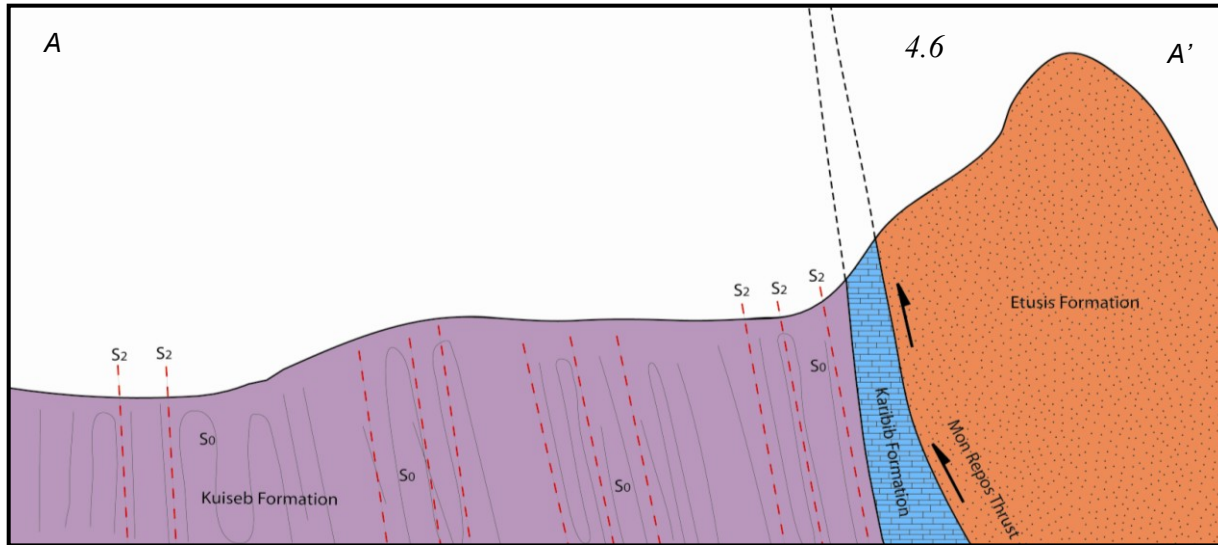


Figure 4.6, Cross-section displaying the steeply dipping/overtuned nature of the southern limb of the Kransberg syncline. The Kuisieb Formation has been intruded by multiple granite plutons; these will be discussed in Chapter 5.

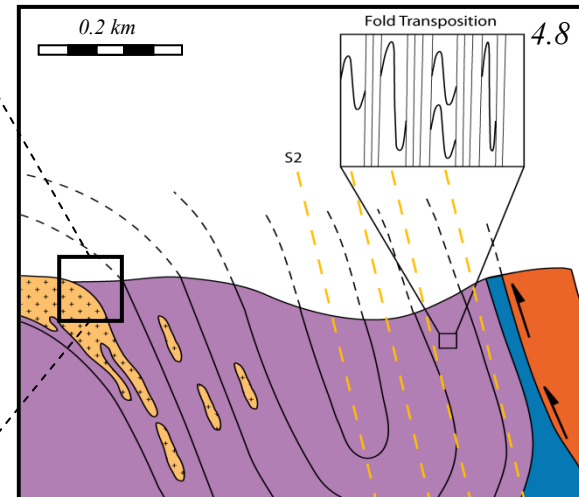
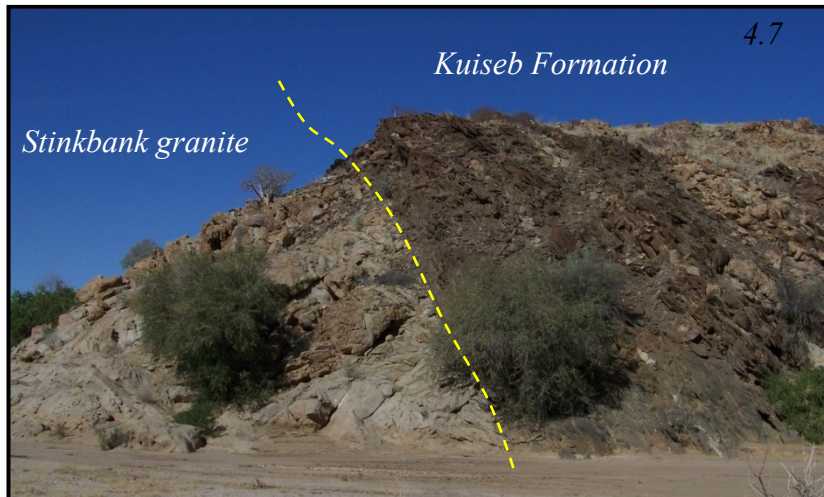


Figure 4.7 and 4.8, cross-section drawn through the southern limb of the Kransberg syncline, illustrating the intruding Stinkbank granite. The contact between the Kuisieb wall-rocks and the granite is concordant (4.8). The cross-section shows an increase of bedding transposition towards the contact between the Kuisieb-, Karibib- and Etusis Formation.

Along the SE limb of the Kransberg syncline, marbles of the Karibib Formation are juxtaposed against rocks of the much older Etusis Formation. There is no trace of rocks of the Chuos, Spes Bona, Okawayo, or Oberwasser Formations that are typically developed between Etusis and Karibib Formation, merely 10 km to the NE along strike of this contact (*e.g. Smith, 1965; Johnson, 2005*). In the southern part of domain 1, between coordinates 22°11'27.28"S, 15°21'16.04"E and 22°12'44.35"S, 15°19'46.50"E (Appendix 1), the Etusis and Karibib Formations are interbedded. The marbles of the Karibib Formation are highly strained, containing slivers of red quartzites and arkoses of the Etusis Formation that range in thickness from merely 50 cm up to blocks of 15-20 m (Figure 3.3, Chapter 3). The interlayering between the Karibib and Etusis Formation describes a progression over ca. 250 m, from SE to NW, perpendicular to the strike of the sequence. Massive quartzites and arkoses with thin (< 2m), interlayered marbles are developed in the SE. These are overlain by a zone of intensely veined and boudinaged quartzites separated by anastomosing marble bands in approximately equal amounts. Structurally higher, isolated, elongated fragments of the Etusis Formation are wrapped by grey-white banded marbles. The juxtaposition and structural imbrication of the two formations and the highly-strained nature of this contact suggests that this contact is structural. Importantly, this contact is the SW continuation of the Mon Repos Thrust Zone that has been mapped by Johnson (2005) on the SE limb of the Usakos Dome, some 10-20 km to the NE and by Kisters et al. (2004) in the Karibib area, more than 35km along strike.

Rocks of the Kuiseb Formation are intruded by decimetre- to meter-wide sills and, less commonly, cross-cutting dykes. These will be discussed in more detail in Chapter 5. However, the predominantly coarse-grained, feldspar-dominated sills are commonly boudinaged and, to a lesser extent, folded, thus providing good strain markers in the rheologically relatively homogeneous schist sequence (Figure 4.11). Boudinage is almost exclusively of a chocolate-tablet type ( $X=Y \gg Z$ , with  $X \geq Y \geq Z$ ), indicating a large-layer normal component of flattening and stretching within the plane of the foliation ( $S_1/S_2$ ). Boudinage is symmetrical, suggesting a subhorizontal, NW-SE directed, largely coaxial flattening strain. This corresponds to the regional NW-SE shortening strain documented from this part of the sCZ (*e.g. Poli and Oliver, 2001, Kisters et al., 2004; Johnson et al., 2006a*), responsible for the formation of regional-scale NE-trending folds and NW-verging thrusts. The only case of three-dimensional boudinage ( $X > Y > Z$ ) was observed in the highly-strained interlayered marble-quartzite sequence that marks the

contact between the Karibib and Etusis Formation (Figure 4.12). In this case, boudin orientation and geometry indicated a steep stretch (X) and shallow SE plunging intermediate strain axis (Y, long axis of boudins), developed during NW-SE subhorizontal shortening (Z). Further examples of boudinage are shown in figures 4.13 and 4.14.



*Figure 4.9*, Oblique view of refolded foliation ( $S_1$ ). Bedding is impossible to identify because of the lack of good marker horizons.

*Figure 4.10*,  $S_1$  foliation crenulated by  $F_{2d}$  folds. Plunges of  $F_{2c}$  and  $F_{2d}$  folds are at various angles towards the NE and SW. This area of intense transposition and crenulation folding is almost devoid of granite and pegmatite sheets.

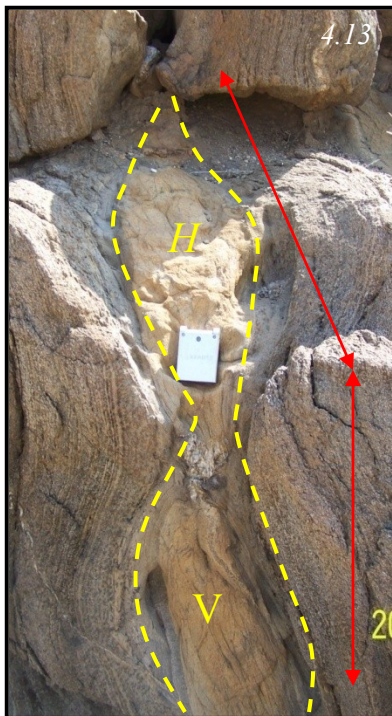


Figure 4.11, Six steeply-dipping granitic sills. Two show no deformation, while the four to the right of the image have undergone boudinage.

Figure 4.12, Bedding plane showing three-dimensional boudinage (i.e.  $X > Y > Z$ ) of Etusis quartzites (red) against marbles of the Karibib Formation (left-hand side of photo). The photo shows the shallowly-plunging long axes of the boudins and necklines (indicating Y) and the layer has undergone layer-normal shortening (Z) and steep stretch (X), normal to the necklines. Photo was taken in the immediate footwall of the Mon-Repos Thrust.

Figure 4.13, An oblique view of chocolate tablet boudinage. The two stretching components, vertical (V) and horizontal (H) have been indicated on the image.

Figure 4.14, Plan view of a granite sill that has undergone stretching and boudinage.

## 4.6 Domain 2

### 4.6.1 Wall-rock Structure

Domain 2 (Figure 4.15) is a structurally complex domain. It represents the SW hinge zone of the first-order fold of the Kransberg Syncline, directly juxtaposed against the NE-plunging basement-cored Namibfontein dome to the SW (*Smith, 1965; Kröner, 1984; Poli and Oliver, 2001*). It also coincides with the SW termination of the Stinkbank granite. In this SW hinge, rocks of the Kuiseb Formation rotate to NW – SE trends. Dips of  $S_0$  and  $S_1$  in the schists are at moderate- to steep angles ( $40\text{-}80^\circ$ ) to the S, SW and NW, wrapping paraconformably around the contact with the Stinkbank granite and corresponding to the overall SW-ward convex outcrop pattern described by the granite wall-rock contact. Hence, the SW hinge of the Kransberg Syncline is actually developed as a moderately SW plunging antiform, cored by rocks of the Stinkbank granite. The opposite plunges of the Kransberg antiformal syncline in the NE and the Namibfontein dome in the SW leads to a NW trending synformal structure between the two NE trending antiforms, here referred to as the Safier synform (based on the farm Safier to the immediate NE). The intervening Safier synform terminates into or merges with NE trending  $F_2$  synforms, that are developed parallel to the dome structures and the overall NE trending structural  $D_2$  grain of the Damara Belt. Fold interference between the three, high-angle synformal structures leads to the formation of two bedding-triple points at the lateral termination of the Safier synform around coordinates  $22^\circ 11' 43.79''\text{S}$ ;  $15^\circ 19' 56.59''\text{E}$  and  $22^\circ 10' 50.70''\text{S}$ ;  $15^\circ 18' 57.31''\text{E}$  (Figure 4.16). The triple points are characterized by the plunge of fold axes as well as stretching lineations towards the centre of these funnel-shaped troughs (Figure 4.16).

Probable formation mechanisms and the regional significance of the bedding-triple points between regional-scale dome structures have been discussed by Poli and Oliver (*2001*). Important for an understanding of the wall-rock structures with regard to the emplacement of the Stinkbank granite are the following observations.

Apart from the first-order  $F_2$  antiform,  $D_2$  related structures, such as the  $S_2$  foliation, parasitic  $F_2$  folds or bedding transposition by  $F_2$  folds are not observed in domain 2. The bedding-parallel  $S_1$  foliation is, in contrast, well developed. This is in contrast to domain 1, where  $D_2$  related structures and fabrics dominate the area. The moderately SW dipping rocks of the Kuiseb Formation are also intruded by abundant bedding-parallel granite sheets, but the sills are commonly not boudinaged in the hinge of the  $F_2$  Kransberg antiformal syncline.

Domain 2

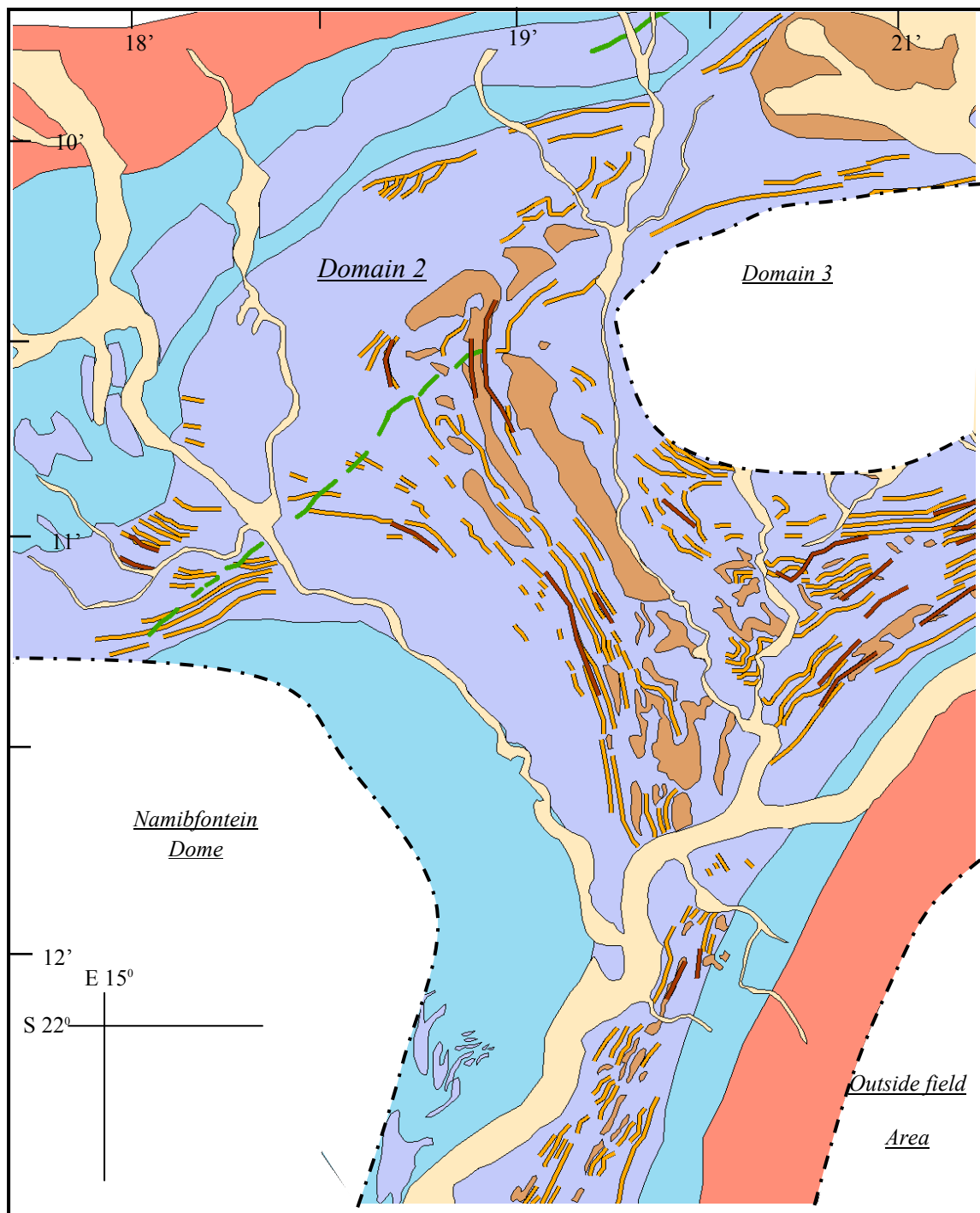


Figure 4.15, Outline of Domain 2, covering the SW closure of the Kransberg Syncline. The closure is described as being a synclinal antiform, with the Stinkbank granite coring it. Note the abundance of granite sills in the Kuiseb Formation overlying the granite- wall-rock contact and reorientation of sills parallel to contact.

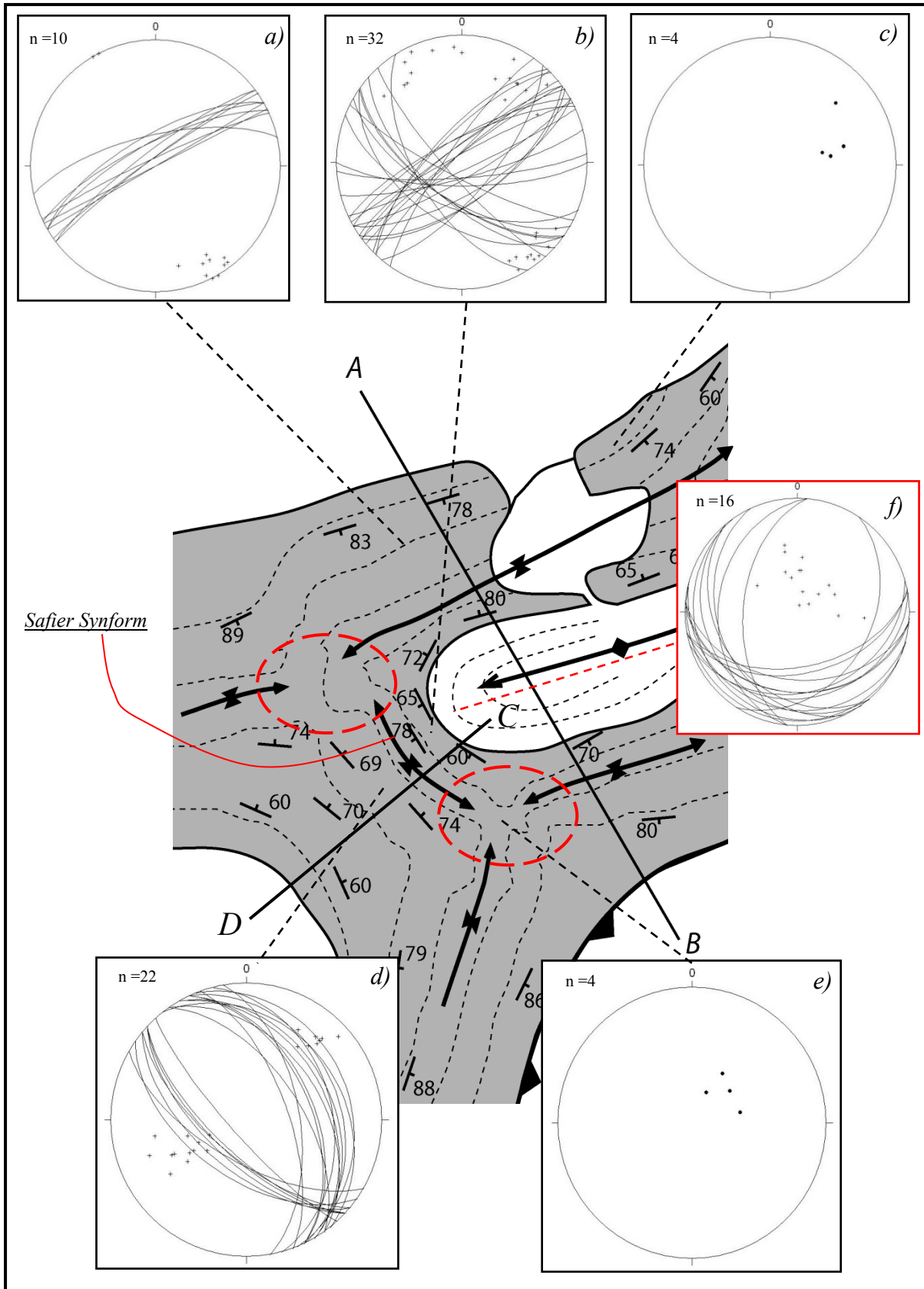


Figure 4.16, Form line map of Domain 2. The two triple-point junctions are easily seen (red dashed circles) and represent the interference of three synforms at one central point. a) Planes and poles of bedding,  $S_0/S_1$  illustrate the subvertical nature of the N-limb of the Kransberg syncline. b) Planes and poles of bedding,  $S_0/S_1$  illustrate the antiformal nature of the SW closure of the Kransberg syncline. Stereonets c) and e) represent fold plunges of  $F_2$  folds. d) Planes and poles of bedding  $S_0/S_1$ , found in the Safier synform. f) Planes and poles to planes of the shallowly dipping internal contacts between the medium grained leucogranite and the fine grained leucogranite. This contact is paraconformable with respect to the granite<sup>41</sup> wall-rock contact.

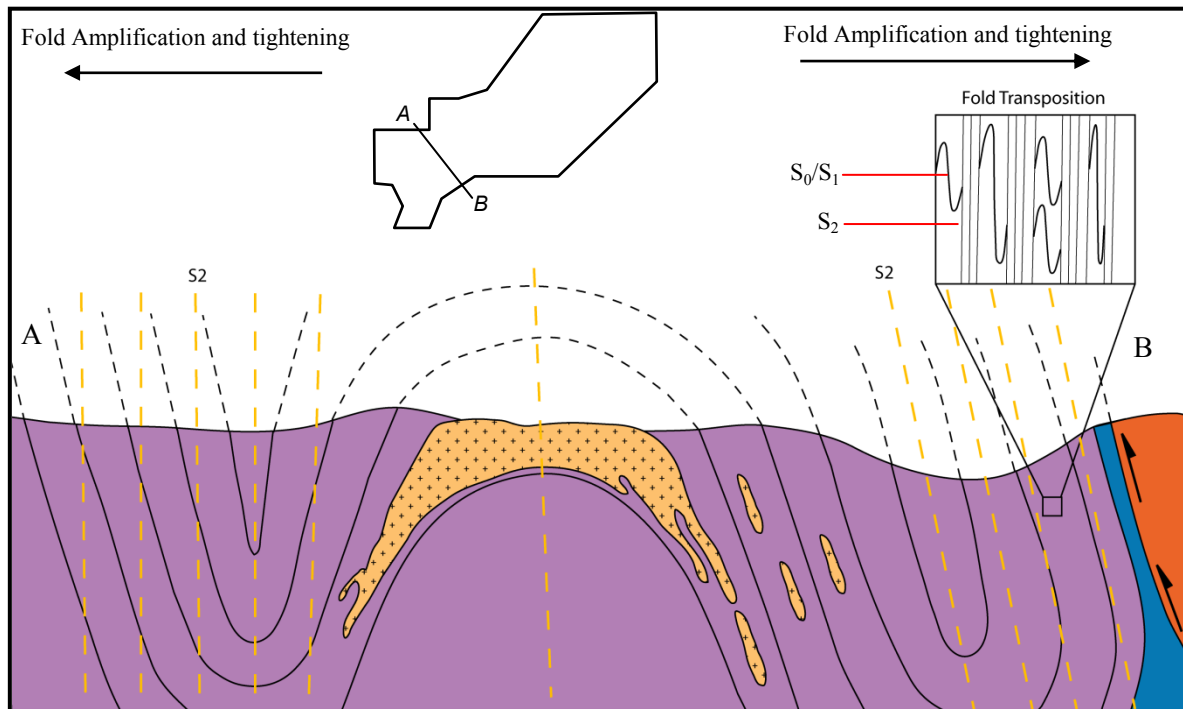
The (D<sub>2</sub>) boudinage of sills is more common in the far SE and NW of domain 2, where the rocks assume NE trends again. Close to bedding-triple junctions, originally boudinaged sills undergo a refolding, indicated by the shortening of original interboudin spaces and initially undeformed sills are folded (Figure 4.17). This suggests a relatively late-stage formation of the bedding-triple points.

Cross-section A-B, through the SW closure of the Kransberg syncline is illustrated in Figure 4.18, a. The cross section shows the amplification and tightening of folding with decreasing distance from the proposed continuation of the MRTZ. Figure 4.18, b is a longitudinal section C-D, drawn through the SW closure of the Stinkbank granite. It illustrates the antiformal nature of the SW closure of the Kransberg syncline.



*Figure 4.17*, Oblique view of a granitic sill that has been boudinaged and refolded. The boudin necks have been forced to close during the later folding, indicating earlier, layer-parallel boudinage and later refolding by an F2 fold.

***Cross section, A-B, through Domain 2, the southern closure of the Kransberg Syncline***



***Longitudinal section, C-D, through the southern closure of the Kransberg Syncline***

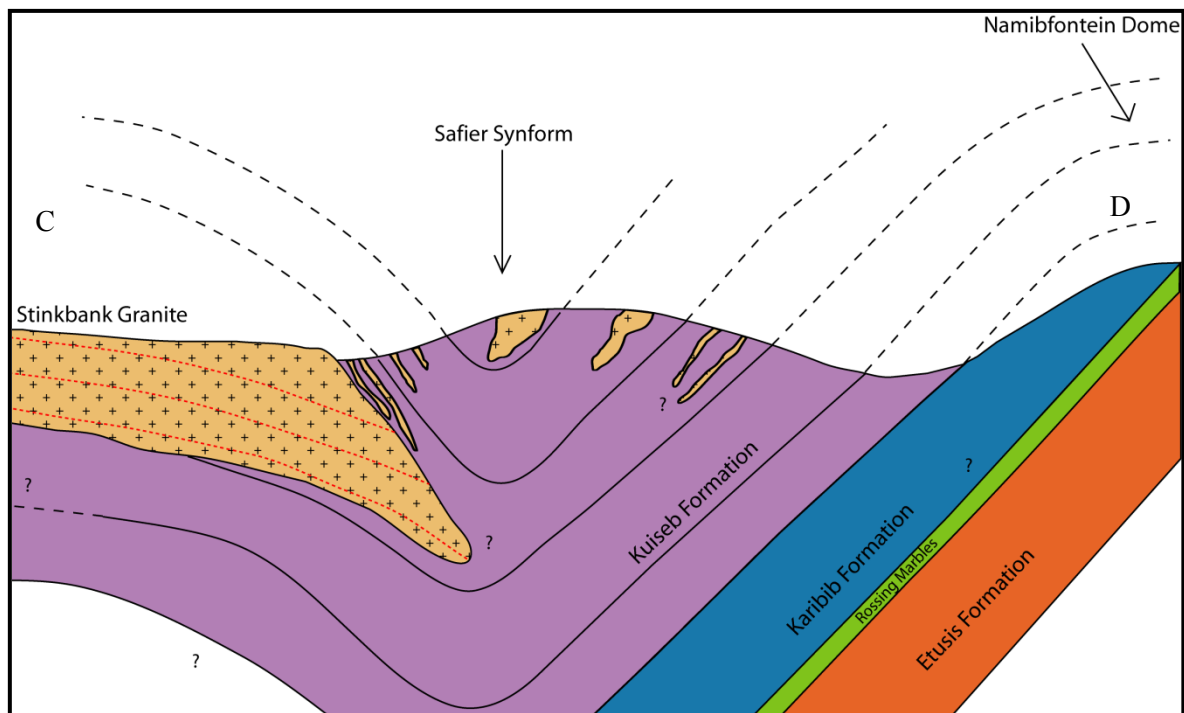


Figure 4.18 a) cross-sectional view of SW closure of the Kransberg syncline. Dips of  $S_0$  and  $S_1$  in the schists are at moderate- to steep angles (40-80), wrapping paraconformably around the contact with the Stinkbank granite. An increase in bedding transposition, fold amplification and tightening of folding is recorded closer to the juxtaposition of the Karibib- and Etusis Formation. The shape of the pluton will be discussed in Chapter 5.

b) Longitudinal section through the SW closure. The closure is described as being an antiformal syncline, cored by the Stinkbank granite body. The Safier synform is the centre point between the southern closure antiform and the Namibfontein dome mapped by Poli and Oliver (2001).